Computers and Structures 89 (2011) 1681–1696

Contents lists available at ScienceDirect

Computers and Structures

journal homepage: www.elsevier.com/locate/compstruc

Geometrically induced stress singularities in a piezoelectric body of revolution

C.S. Huang *, C.N. Hu

Department of Civil Engineering, National Chiao Tung University, 1001 Ta-Hsueh Rd., Hsinchu 30050, Taiwan

ARTICLE INFO

Article history:
Received 8 December 2010
Accepted 26 April 2011
Available online 28 May 2011

Keywords:
Piezoelectric bodies of revolution
Electroelastic singularities
Eigenfunction expansion approach
Asymptotic solutions

ABSTRACT

An eigenfunction expansion approach is combined with a power series solution technique to establish the asymptotic solutions for geometrically induced electroelastic singularities in a piezoelectric body of revolution, with its direction of polarization not parallel to the axis of revolution. The asymptotic solutions are obtained by directly solving the three-dimensional equilibrium and Maxwell's equations in terms of displacement components and electric potential. When the direction of polarization is not along the axis of revolution, the assumption of axisymmetric deformation that is often made in the published literature is not valid, and the direction of polarization and the circular coordinate variable can substantially affect the singularities. The numerical results related to singularity orders are shown in graphical form for bodies of revolution that comprise a single material (PZT-4 or PZT-5H) or bonded piezo/piezo (PZT-4/PZT-5H) or piezo/isotropic elastic (PZT-4/Al or PZT-5H/Al) materials. This is the first study to present results for the direction of polarization not along the axis of revolution.

1. Introduction

Piezoelectric materials have been extensively adopted to manufacture various sensors, conductors, actuators, resonators, oscillators and monitors, and have an important role in smart structures. A comprehensive understanding of the electroelastic singularities that are induced by geometry is valuable in optimizing the design of piezoelectric components, and analyzing their failure. An accurate numerical analysis of problems that involve stress singularities depends on knowledge of such stress singularity behaviors. The two typical geometries that are commonly considered in the literature on geometrically induced stress singularities are wedges and bodies of revolution.

Only a few studies have examined the eletroelastic singularity behaviors at the vertex of a piezoelectric wedge, even though considerable research has been done on elastic wedges, using various plate theories and 3D elasticity theory ([1–13], for example). Xu and Rajapakse [14] extended Lekhnitskii's complex potential functions to study plane problems of piezoelectric wedges and multi-material wedges involving piezoelectrics, while Hwu and Ikeda [15] proposed an extended Stroh formulation. Chue and Chen [16] presented a decoupled formulation of piezoelectric elasticity based on generalized plane deformation, and this formulation was subsequently adopted to examine antiplane stress singularities in a bi-material piezoelectric wedge [17]. Chen et al. [18] utilized the extended Lekhnitskii formulation to determine the electroelastic singularity behaviors near the apex of a cylindrical polarized piezoelectric wedge.

Numerous analyses of stress singularities for elastic isotropic bodies of revolution are available. Making an assumption of axisymmetric deformation, Zak [19] utilized the Love stress approach [20] to investigate geometrically induced stress singularities in bodies of revolution that were made of a single material, while Li et al. [21,22] adopted the Love stress approach and Boussinesq's solution [23], respectively, to obtain the stress field near the bond edge of a bi-material body of revolution. Ting et al. [24] presented eigenfunctions at a singular point of a body of revolution made of transversely isotropic material. Without assuming axisymmetric deformation, Huang and Leissa [25] presented three-dimensional sharp corner displacement functions for bodies of revolution, and further studied the geometrically induced stress singularities in bimaterial bodies of revolution [26].

A review of the literature reveals only two investigations that considered electroelastic singularities in a piezoelectric body of revolution, based on axisymmetric deformation assumptions. To perform stress singularity analysis of axisymmetric piezoelectric bonded structures, Xu and Mutoh [27] adopted the general solutions for coupled equations for piezoelectric material that was developed by Ding et al. [28], while Li et al. [29] extended the method proposed by Ting et al. [24] for an elastic material. These solutions consist of four and three quasi-harmonic functions, respectively. In these two works, the direction of polarization of the piezoelectric material was assumed to be along the axis of revolution.

The main purpose of the present research is to develop an asymptotic solution for the eletroelastic singularities in a

* Corresponding author. Tel.: +886 3 5712121x54962.
E-mail address: cshuang@mail.nctu.edu.tw (C.S. Huang).

0045-7949/$ - see front matter © 2011 Elsevier Ltd. All rights reserved.
doi:10.1016/j.compstruc.2011.04.010

piezoelectric body of revolution without assuming that the direction of polarization of the material is along the axis of revolution. When a piezoelectric material is considered to be transversely isotropic, and the axis of material symmetry is not parallel to the axis of revolution, the assumption of axisymmetric deformation is no longer valid. An eigenfunction expansion approach combined with a power series method is adopted to solve the equilibrium and Maxwell's equations in terms of mechanical displacement components and electric potential. The correctness of the proposed solution is confirmed by comparing the present results with the published results in cases in which the direction of polarization is along the axis of revolution. Analyses are performed on bodies that comprise a single piezoelectric material (PZT-4 or PZT-5H), bonded piezo/piezo (PZT-4/PZT-5H) or piezo/isotropic elastic (PZT-4/Al or PZT-5H/Al) materials. The effects of polarization orientation, material type (s) and boundary conditions on the singularity orders are comprehensively examined. This study is the first to present numerical results for a direction of polarization that is not along the axis of revolution.

2. Basic equations

Consider a body of revolution made of a piezoelectric material polarized along the direction $\bar{Z}$, which makes an angle γ with the axis of revolution Z (Fig. 1). Although Fig. 1 displays a bi-material body of revolution, a body of a single material will be first considered in the following development of basic equations and solutions. The solutions are then easily extended to a bimaterial body. Define two Cartesian coordinate systems (X,Y,Z) and $(\bar{X},\bar{Y},\bar{Z})$, where Y and $\bar{Y}$ axes are coincidental. A cylindrical coordinate system (r,θ,Z) (Fig. 1) can be conveniently used to solve problems of bodies of revolution. Without body force and charges, the equilibrium and Maxwell's equations in terms of stress components (σ_{ij}) and electric displacements (D_i) in the cylindrical coordinate system are [30].

$$\frac{\partial \sigma_{rr}}{\partial r}+\frac{1}{r}\frac{\partial \sigma_{r\theta}}{\partial \theta}+\frac{\partial \sigma_{rz}}{\partial z}+\frac{(\sigma_{rr}-\sigma_{\theta\theta})}{r}=0, \quad (1a)$$

$$\frac{\partial \sigma_{r\theta}}{\partial r}+\frac{1}{r}\frac{\partial \sigma_{\theta\theta}}{\partial \theta}+\frac{\partial \sigma_{\theta z}}{\partial z}+2\frac{\sigma_{r\theta}}{r}=0, \quad (1b)$$

$$\frac{\partial \sigma_{rz}}{\partial r}+\frac{1}{r}\frac{\partial \sigma_{\theta z}}{\partial \theta}+\frac{\partial \sigma_{zz}}{\partial z}+\frac{\sigma_{rz}}{r}=0, \quad (1c)$$

$$\frac{1}{r}\frac{\partial (rD_r)}{\partial r}+\frac{1}{r}\frac{\partial D_\theta}{\partial \theta}+\frac{\partial D_z}{\partial z}=0. \quad (1d)$$

The constitutive equations of a piezoelectric material possessing transversely isotropic property on $\bar{X}-\bar{Y}$ plane are expressed in $(\bar{X},\bar{Y},\bar{Z})$ as

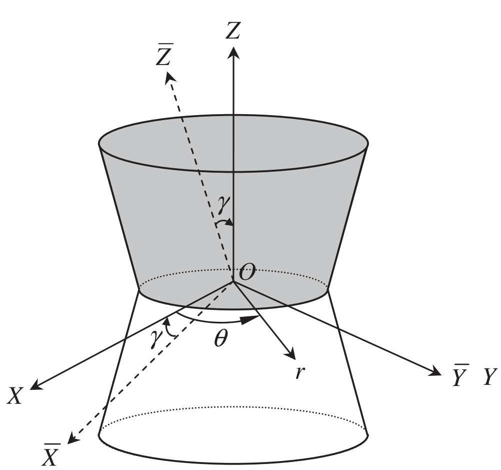

Fig. 1. Bi-material body of revolution with a sharp corner.

$$\{\bar{\sigma}\}=[\bar{c}]\{\bar{\varepsilon}\}-[\bar{e}]^T\{\bar{E}\}, \quad (2a)$$

$$\{\bar{D}\}=[\bar{e}]\{\bar{\varepsilon}\}+[\bar{\eta}]\{\bar{E}\}, \quad (2b)$$

where

$$\{\bar{\sigma}\}=\{\sigma_{\bar{x}\bar{x}} \quad \sigma_{\bar{y}\bar{y}} \quad \sigma_{\bar{z}\bar{z}} \quad \sigma_{\bar{y}\bar{z}} \quad \sigma_{\bar{z}\bar{x}} \quad \sigma_{\bar{x}\bar{y}}\}^T,$$

$$\{\bar{\varepsilon}\}=\{\varepsilon_{\bar{x}\bar{x}} \quad \varepsilon_{\bar{y}\bar{y}} \quad \varepsilon_{\bar{z}\bar{z}} \quad 2\varepsilon_{\bar{y}\bar{z}} \quad 2\varepsilon_{\bar{z}\bar{x}} \quad 2\varepsilon_{\bar{x}\bar{y}}\}^T,$$

$$\{\bar{D}\}=\{D_{\bar{x}}\ D_{\bar{y}}\ D_{\bar{z}}\}^T, \quad \{\bar{E}\}=\{E_{\bar{x}}\ E_{\bar{y}}\ E_{\bar{z}}\}^T,$$

$$[\bar{c}]=\begin{bmatrix}\bar{c}_{11} & \bar{c}_{12} & \bar{c}_{13} & 0 & 0 & 0\\ \bar{c}_{12} & \bar{c}_{11} & \bar{c}_{13} & 0 & 0 & 0\\ \bar{c}_{13} & \bar{c}_{13} & \bar{c}_{33} & 0 & 0 & 0\\ 0 & 0 & 0 & \bar{c}_{44} & 0 & 0\\ 0 & 0 & 0 & 0 & \bar{c}_{44} & 0\\ 0 & 0 & 0 & 0 & 0 & \frac{\bar{c}_{11}-\bar{c}_{12}}{2}\end{bmatrix},$$

$$[\bar{e}]=\begin{bmatrix}0 & 0 & 0 & 0 & \bar{e}_{15} & 0\\ 0 & 0 & 0 & \bar{e}_{15} & 0 & 0\\ \bar{e}_{31} & \bar{e}_{31} & \bar{e}_{33} & 0 & 0 & 0\end{bmatrix},$$

$$[\bar{\eta}]=\begin{bmatrix}\bar{\eta}_{11} & 0 & 0\\ 0 & \bar{\eta}_{11} & 0\\ 0 & 0 & \bar{\eta}_{33}\end{bmatrix}. \quad (3)$$

Transformation among coordinate systems $(\bar{X},\bar{Y},\bar{Z})$, (X,Y,Z) and (r,θ,Z) yields the constitutive equations in (r,θ,Z),

$$\{\sigma\}=[c]\{\varepsilon\}-[e]^T\{E\}, \quad (4a)$$

$$\{D\}=[e]\{\varepsilon\}+[\eta]\{E\}, \quad (4b)$$

where $\{\sigma\}=\{\sigma_{rr} \quad \sigma_{\theta\theta} \quad \sigma_{zz} \quad \sigma_{\theta z} \quad \sigma_{zr} \quad \sigma_{r\theta}\}^T$, $\{\varepsilon\}=\{\varepsilon_{rr} \quad \varepsilon_{\theta\theta} \quad \varepsilon_{zz} \quad 2\varepsilon_{\theta z} \quad 2\varepsilon_{zr} \quad 2\varepsilon_{r\theta}\}^T$

$$\{D\}=\{D_r\ D_\theta\ D_z\}^T, \quad \{E\}=\{E_r\ E_\theta\ E_z\}^T,$$

$$[c]=\begin{bmatrix}c_{11} & c_{12} & c_{13} & c_{14} & c_{15} & c_{16}\\ c_{12} & c_{22} & c_{23} & c_{24} & c_{25} & c_{26}\\ c_{13} & c_{23} & c_{33} & c_{34} & c_{35} & c_{36}\\ c_{14} & c_{24} & c_{34} & c_{44} & c_{45} & c_{46}\\ c_{15} & c_{25} & c_{35} & c_{45} & c_{55} & c_{56}\\ c_{16} & c_{26} & c_{36} & c_{46} & c_{56} & c_{66}\end{bmatrix},$$

$$[e]=\begin{bmatrix}e_{11} & e_{12} & e_{13} & e_{14} & e_{15} & e_{16}\\ e_{21} & e_{22} & e_{23} & e_{24} & e_{25} & e_{26}\\ e_{31} & e_{32} & e_{33} & e_{34} & e_{35} & e_{36}\end{bmatrix},$$

$$[\eta]=\begin{bmatrix}\eta_{11} & \eta_{12} & \eta_{13}\\ \eta_{12} & \eta_{22} & \eta_{23}\\ \eta_{13} & \eta_{23} & \eta_{33}\end{bmatrix}. \quad (5)$$

The components of $[c]$, $[e]$ and $[\eta]$ are related to the components of $[\bar{c}]$, $[\bar{e}]$ and $[\bar{\eta}]$, respectively, and are functions of θ and γ. The relations are given in Appendix A.

From Eqs. (4) and (5) and using strain–displacement relations and electric field-potential relations,

$$\begin{aligned}\sigma_{rr}=&\,c_{11}\frac{\partial u_r}{\partial r}+c_{12}\left(\frac{1}{r}\frac{\partial u_\theta}{\partial \theta}+\frac{u_r}{r}\right)+c_{13}\frac{\partial u_z}{\partial z}\\ &+c_{14}\left(\frac{\partial u_\theta}{\partial z}+\frac{1}{r}\frac{\partial u_z}{\partial \theta}\right)+c_{15}\left(\frac{\partial u_z}{\partial r}+\frac{\partial u_r}{\partial z}\right)\\ &+c_{16}\left(\frac{1}{r}\frac{\partial u_r}{\partial \theta}+\frac{\partial u_\theta}{\partial r}-\frac{u_\theta}{r}\right)+e_{11}\frac{\partial \phi}{\partial r}+e_{21}\frac{1}{r}\frac{\partial \phi}{\partial \theta}+e_{31}\frac{\partial \phi}{\partial z},\end{aligned} \quad (6a)$$

$$\sigma_{\theta\theta} = c_{12}\frac{\partial u_r}{\partial r} + c_{22}\left(\frac{1}{r}\frac{\partial u_\theta}{\partial \theta} + \frac{u_r}{r}\right) + c_{23}\frac{\partial u_z}{\partial z} + c_{24}\left(\frac{\partial u_\theta}{\partial z} + \frac{1}{r}\frac{\partial u_z}{\partial \theta}\right) + c_{25}\left(\frac{\partial u_z}{\partial r} + \frac{\partial u_r}{\partial z}\right) + c_{26}\left(\frac{1}{r}\frac{\partial u_r}{\partial \theta} + \frac{\partial u_\theta}{\partial r} - \frac{u_\theta}{r}\right) + e_{12}\frac{\partial \phi}{\partial r} + e_{22}\frac{1}{r}\frac{\partial \phi}{\partial \theta} + e_{32}\frac{\partial \phi}{\partial z}, \tag{6b}$$

$$\sigma_{zz} = c_{13}\frac{\partial u_r}{\partial r} + c_{23}\left(\frac{1}{r}\frac{\partial u_\theta}{\partial \theta} + \frac{u_r}{r}\right) + c_{33}\frac{\partial u_z}{\partial z} + c_{34}\left(\frac{\partial u_\theta}{\partial z} + \frac{1}{r}\frac{\partial u_z}{\partial \theta}\right) + c_{35}\left(\frac{\partial u_z}{\partial r} + \frac{\partial u_r}{\partial z}\right) + c_{36}\left(\frac{1}{r}\frac{\partial u_r}{\partial \theta} + \frac{\partial u_\theta}{\partial r} - \frac{u_\theta}{r}\right) + e_{13}\frac{\partial \phi}{\partial r} + e_{23}\frac{1}{r}\frac{\partial \phi}{\partial \theta} + e_{33}\frac{\partial \phi}{\partial z}, \tag{6c}$$

$$\sigma_{z\theta} = c_{14}\frac{\partial u_r}{\partial r} + c_{24}\left(\frac{1}{r}\frac{\partial u_\theta}{\partial \theta} + \frac{u_r}{r}\right) + c_{34}\frac{\partial u_z}{\partial z} + c_{44}\left(\frac{\partial u_\theta}{\partial z} + \frac{1}{r}\frac{\partial u_z}{\partial \theta}\right) + c_{45}\left(\frac{\partial u_z}{\partial r} + \frac{\partial u_r}{\partial z}\right) + c_{46}\left(\frac{1}{r}\frac{\partial u_r}{\partial \theta} + \frac{\partial u_\theta}{\partial r} - \frac{u_\theta}{r}\right) + e_{14}\frac{\partial \phi}{\partial r} + e_{24}\frac{1}{r}\frac{\partial \phi}{\partial \theta} + e_{34}\frac{\partial \phi}{\partial z}, \tag{6d}$$

$$\sigma_{zr} = c_{15}\frac{\partial u_r}{\partial r} + c_{25}\left(\frac{1}{r}\frac{\partial u_\theta}{\partial \theta} + \frac{u_r}{r}\right) + c_{35}\frac{\partial u_z}{\partial z} + c_{45}\left(\frac{\partial u_\theta}{\partial z} + \frac{1}{r}\frac{\partial u_z}{\partial \theta}\right) + c_{55}\left(\frac{\partial u_z}{\partial r} + \frac{\partial u_r}{\partial z}\right) + c_{56}\left(\frac{1}{r}\frac{\partial u_r}{\partial \theta} + \frac{\partial u_\theta}{\partial r} - \frac{u_\theta}{r}\right) + e_{15}\frac{\partial \phi}{\partial r} + e_{25}\frac{1}{r}\frac{\partial \phi}{\partial \theta} + e_{35}\frac{\partial \phi}{\partial z}, \tag{6e}$$

$$\sigma_{r\theta} = c_{16}\frac{\partial u_r}{\partial r} + c_{26}\left(\frac{1}{r}\frac{\partial u_\theta}{\partial \theta} + \frac{u_r}{r}\right) + c_{36}\frac{\partial u_z}{\partial z} + c_{46}\left(\frac{\partial u_\theta}{\partial z} + \frac{1}{r}\frac{\partial u_z}{\partial \theta}\right) + c_{56}\left(\frac{\partial u_z}{\partial r} + \frac{\partial u_r}{\partial z}\right) + c_{66}\left(\frac{1}{r}\frac{\partial u_r}{\partial \theta} + \frac{\partial u_\theta}{\partial r} - \frac{u_\theta}{r}\right) + e_{16}\frac{\partial \phi}{\partial r} + e_{26}\frac{1}{r}\frac{\partial \phi}{\partial \theta} + e_{36}\frac{\partial \phi}{\partial z}, \tag{6f}$$

$$D_r = e_{11}\frac{\partial u_r}{\partial r} + e_{12}\left(\frac{1}{r}\frac{\partial u_\theta}{\partial \theta} + \frac{u_r}{r}\right) + e_{13}\frac{\partial u_z}{\partial z} + e_{14}\left(\frac{\partial u_\theta}{\partial z} + \frac{1}{r}\frac{\partial u_z}{\partial \theta}\right) + e_{15}\left(\frac{\partial u_z}{\partial r} + \frac{\partial u_r}{\partial z}\right) + e_{16}\left(\frac{1}{r}\frac{\partial u_r}{\partial \theta} + \frac{\partial u_\theta}{\partial r} - \frac{u_\theta}{r}\right) - \eta_{11}\frac{\partial \phi}{\partial r} - \eta_{12}\frac{1}{r}\frac{\partial \phi}{\partial \theta} - \eta_{13}\frac{\partial \phi}{\partial z}, \tag{6g}$$

$$D_\theta = e_{21}\frac{\partial u_r}{\partial r} + e_{22}\left(\frac{1}{r}\frac{\partial u_\theta}{\partial \theta} + \frac{u_r}{r}\right) + e_{23}\frac{\partial u_z}{\partial z} + e_{24}\left(\frac{\partial u_\theta}{\partial z} + \frac{1}{r}\frac{\partial u_z}{\partial \theta}\right) + e_{25}\left(\frac{\partial u_z}{\partial r} + \frac{\partial u_r}{\partial z}\right) + e_{26}\left(\frac{1}{r}\frac{\partial u_r}{\partial \theta} + \frac{\partial u_\theta}{\partial r} - \frac{u_\theta}{r}\right) - \eta_{12}\frac{\partial \phi}{\partial r} - \eta_{22}\frac{1}{r}\frac{\partial \phi}{\partial \theta} - \eta_{23}\frac{\partial \phi}{\partial z}, \tag{6h}$$

$$D_z = e_{31}\frac{\partial u_r}{\partial r} + e_{32}\left(\frac{1}{r}\frac{\partial u_\theta}{\partial \theta} + \frac{u_r}{r}\right) + e_{33}\frac{\partial u_z}{\partial z} + e_{34}\left(\frac{\partial u_\theta}{\partial z} + \frac{1}{r}\frac{\partial u_z}{\partial \theta}\right) + e_{35}\left(\frac{\partial u_z}{\partial r} + \frac{\partial u_r}{\partial z}\right) + e_{36}\left(\frac{1}{r}\frac{\partial u_r}{\partial \theta} + \frac{\partial u_\theta}{\partial r} - \frac{u_\theta}{r}\right) - \eta_{13}\frac{\partial \phi}{\partial r} - \eta_{23}\frac{1}{r}\frac{\partial \phi}{\partial \theta} - \eta_{33}\frac{\partial \phi}{\partial z}, \tag{6i}$$

where the electric potential, ϕ, is related to the electric field by,

$$E_r = -\frac{\partial \phi}{\partial r}, \quad E_\theta = -\frac{1}{r}\frac{\partial \phi}{\partial \theta} \quad \text{and} \quad E_z = -\frac{\partial \phi}{\partial z}.$$

Substituting Eqs. (6) into Eqs. (1) yields the following equilibrium and Maxwell's equations in terms of displacement components and electric potential;

$$\begin{aligned}
&\Bigg[c_{11}\frac{\partial^2}{\partial r^2} + c_{55}\frac{\partial^2}{\partial z^2} + \left(c_{11} + \frac{\partial c_{16}}{\partial \theta}\right)\frac{\partial}{r\partial r} + \left(c_{15} + \frac{\partial c_{56}}{\partial \theta}\right)\frac{\partial}{r\partial z} \\
&+ \frac{\partial c_{66}}{\partial \theta}\frac{\partial}{r^2\partial \theta} + 2c_{16}\frac{\partial^2}{r\partial r\partial \theta} + 2c_{56}\frac{\partial^2}{r\partial \theta\partial z} + 2c_{15}\frac{\partial^2}{\partial r\partial z} \\
&+ \left(-c_{22} + \frac{\partial c_{26}}{\partial \theta} + c_{66}\frac{\partial^2}{\partial \theta^2}\right)\frac{1}{r^2}\Bigg]u_r + \Bigg[c_{16}\frac{\partial^2}{\partial r^2} + c_{45}\frac{\partial^2}{\partial z^2} \\
&+ \left(-c_{26} + \frac{\partial c_{66}}{\partial \theta}\right)\frac{\partial}{r\partial r} + \left(c_{14} - c_{24} - c_{56} + \frac{\partial c_{46}}{\partial \theta}\right)\frac{\partial}{r\partial z} \\
&+ \left(-c_{22} - c_{66} + \frac{\partial c_{26}}{\partial \theta}\right)\frac{\partial}{r^2\partial \theta} + (c_{12} + c_{66})\frac{\partial^2}{r\partial r\partial \theta} \\
&+ \left(c_{25} + c_{46}\right)\frac{\partial^2}{r\partial \theta\partial z} + (c_{14} + c_{56})\frac{\partial^2}{\partial r\partial z} \\
&+ \left(c_{26} - \frac{\partial c_{66}}{\partial \theta} + c_{26}\frac{\partial^2}{\partial \theta^2}\right)\frac{1}{r^2}\Bigg]u_\theta \\
&+ \Bigg[c_{15}\frac{\partial^2}{\partial r^2} + c_{35}\frac{\partial^2}{\partial z^2} + \left(c_{15} - c_{25} + \frac{\partial c_{56}}{\partial \theta}\right)\frac{\partial}{r\partial r} \\
&+ \left(c_{13} - c_{23} + \frac{\partial c_{36}}{\partial \theta}\right)\frac{\partial}{r\partial z} + \left(-c_{24} + \frac{\partial c_{46}}{\partial \theta}\right)\frac{\partial}{r^2\partial \theta} \\
&+ \left(c_{14} + c_{56}\right)\frac{\partial^2}{r\partial r\partial \theta} + (c_{36} + c_{45})\frac{\partial^2}{r\partial \theta\partial z} \\
&+ \left(c_{13} + c_{55}\right)\frac{\partial^2}{\partial r\partial z} + c_{46}\frac{\partial^2}{r^2\partial \theta^2}\Bigg]u_z \\
&+ \Bigg[e_{11}\frac{\partial^2}{\partial r^2} + e_{35}\frac{\partial^2}{\partial z^2} + \left(e_{11} - e_{12} + \frac{\partial e_{16}}{\partial \theta}\right)\frac{\partial}{r\partial r} \\
&+ \left(e_{31} - e_{32} + \frac{\partial e_{36}}{\partial \theta}\right)\frac{\partial}{r\partial z} + \left(-e_{22} + \frac{\partial e_{26}}{\partial \theta}\right)\frac{\partial}{r^2\partial \theta} \\
&+ (e_{16} + e_{21})\frac{\partial^2}{r\partial r\partial \theta} + (e_{25} + e_{36})\frac{\partial^2}{r\partial \theta\partial z} \\
&+ (e_{31} + e_{15})\frac{\partial^2}{\partial r\partial z} + e_{26}\frac{\partial^2}{r^2\partial \theta^2}\Bigg]\phi = 0,
\end{aligned} \tag{7a}$$

$$\begin{aligned}
&\Bigg[c_{16}\frac{\partial^2}{\partial r^2} + c_{45}\frac{\partial^2}{\partial z^2} + \left(2c_{16} + c_{26} + \frac{\partial c_{12}}{\partial \theta}\right)\frac{\partial}{r\partial r} + \left(2c_{56} + c_{24} + \frac{\partial c_{25}}{\partial \theta}\right)\frac{\partial}{r\partial z} \\
&+ \left(c_{22} + c_{66} + \frac{\partial c_{26}}{\partial \theta}\right)\frac{\partial}{r^2\partial \theta} + (c_{12} + c_{66})\frac{\partial^2}{r\partial r\partial \theta} + (c_{25} + c_{46})\frac{\partial^2}{r\partial \theta\partial z} \\
&+ (c_{56} + c_{14})\frac{\partial^2}{\partial r\partial z} + \left(c_{26} + \frac{\partial c_{22}}{\partial \theta} + c_{26}\frac{\partial^2}{\partial \theta^2}\right)\frac{1}{r^2}\Bigg]u_r \\
&+ \Bigg[c_{66}\frac{\partial^2}{\partial r^2} + c_{44}\frac{\partial^2}{\partial z^2} + \left(c_{66} + \frac{\partial c_{26}}{\partial \theta}\right)\frac{\partial}{r\partial r} + \left(c_{46} + \frac{\partial c_{24}}{\partial \theta}\right)\frac{\partial}{r\partial z} \\
&+ \left(\frac{\partial c_{22}}{\partial \theta}\right)\frac{\partial}{r^2\partial \theta} + 2c_{26}\frac{\partial^2}{r\partial r\partial \theta} + 2c_{24}\frac{\partial^2}{r\partial \theta\partial z} + 2c_{46}\frac{\partial^2}{\partial r\partial z} \\
&+ \left(-c_{66} - \frac{\partial c_{26}}{\partial \theta} + c_{22}\frac{\partial^2}{\partial \theta^2}\right)\frac{1}{r^2}\Bigg]u_\theta + \Bigg[c_{56}\frac{\partial^2}{\partial r^2} + c_{34}\frac{\partial^2}{\partial z^2} \\
&+ \left(2c_{56} + \frac{\partial c_{25}}{\partial \theta}\right)\frac{\partial}{r\partial r} + \left(2c_{36} + \frac{\partial c_{23}}{\partial \theta}\right)\frac{\partial}{r\partial z} + \left(c_{46} + \frac{\partial c_{24}}{\partial \theta}\right)\frac{\partial}{r^2\partial \theta} \\
&+ (c_{25} + c_{46})\frac{\partial^2}{r\partial r\partial \theta} + (c_{23} + c_{44})\frac{\partial^2}{r\partial \theta\partial z} + (c_{36} + c_{45})\frac{\partial^2}{\partial r\partial z} + c_{24}\frac{\partial^2}{r^2\partial \theta^2}\Bigg]u_z
\end{aligned}$$

$$\begin{aligned}&+\left[e_{16}\frac{\partial^2}{\partial r^2}+e_{34}\frac{\partial^2}{\partial z^2}+\left(2e_{16}+\frac{\partial e_{12}}{\partial\theta}\right)\frac{\partial}{r\partial r}+\left(2e_{36}+\frac{\partial e_{32}}{\partial\theta}\right)\frac{\partial}{r\partial z}\right.\\&+\left(e_{26}+\frac{\partial e_{22}}{\partial\theta}\right)\frac{\partial}{r^2\partial\theta}+(e_{12}+e_{26})\frac{\partial^2}{r\partial r\partial\theta}+(e_{24}+e_{32})\frac{\partial^2}{r\partial\theta\partial z}\\&\left.+(e_{36}+e_{14})\frac{\partial^2}{\partial r\partial z}+e_{22}\frac{\partial^2}{r^2\partial\theta^2}\right]\phi=0,\end{aligned}\tag{7b}$$

$$\begin{aligned}&\left[c_{15}\frac{\partial^2}{\partial r^2}+c_{35}\frac{\partial^2}{\partial z^2}+\left(c_{15}+c_{25}+\frac{\partial c_{14}}{\partial\theta}\right)\frac{\partial}{r\partial r}+\left(c_{23}+c_{55}+\frac{\partial c_{45}}{\partial\theta}\right)\frac{\partial}{r\partial z}\right.\\&+\left(c_{24}+\frac{\partial c_{46}}{\partial\theta}\right)\frac{\partial}{r^2\partial\theta}+(c_{14}+c_{56})\frac{\partial^2}{r\partial r\partial\theta}+(c_{45}+c_{36})\frac{\partial^2}{r\partial\theta\partial z}\\&\left.+(c_{55}+c_{13})\frac{\partial^2}{\partial r\partial z}+\left(\frac{\partial c_{24}}{\partial\theta}+c_{46}\frac{\partial^2}{\partial\theta^2}\right)\frac{1}{r^2}\right]u_r+\left[c_{56}\frac{\partial^2}{\partial r^2}+c_{34}\frac{\partial^2}{\partial z^2}\right.\\&+\left(\frac{\partial c_{46}}{\partial\theta}\right)\frac{\partial}{r\partial r}+\left(c_{45}-c_{36}+\frac{\partial c_{44}}{\partial\theta}\right)\frac{\partial}{r\partial z}+\left(-c_{46}+\frac{\partial c_{24}}{\partial\theta}\right)\frac{\partial}{r^2\partial\theta}\\&+(c_{25}+c_{46})\frac{\partial^2}{r\partial r\partial\theta}+(c_{44}+c_{23})\frac{\partial^2}{r\partial\theta\partial z}+(c_{45}+c_{36})\frac{\partial^2}{\partial r\partial z}\\&\left.+\left(-\frac{\partial c_{46}}{\partial\theta}+c_{24}\frac{\partial^2}{\partial\theta^2}\right)\frac{1}{r^2}\right]u_\theta+\left[c_{55}\frac{\partial^2}{\partial r^2}+c_{33}\frac{\partial^2}{\partial z^2}+\left(c_{55}+\frac{\partial c_{45}}{\partial\theta}\right)\frac{\partial}{r\partial r}\right.\\&+\left(c_{35}+\frac{\partial c_{34}}{\partial\theta}\right)\frac{\partial}{r\partial z}+\left(\frac{\partial c_{44}}{\partial\theta}\right)\frac{\partial}{r^2\partial\theta}+2c_{45}\frac{\partial^2}{r\partial r\partial\theta}+2c_{34}\frac{\partial^2}{r\partial\theta\partial z}\\&\left.+2c_{35}\frac{\partial^2}{\partial r\partial z}+c_{44}\frac{\partial^2}{r^2\partial\theta^2}\right]u_z+\left[e_{15}\frac{\partial^2}{\partial r^2}+e_{33}\frac{\partial^2}{\partial z^2}+\left(e_{15}+\frac{\partial e_{14}}{\partial\theta}\right)\frac{\partial}{r\partial r}\right.\\&+\left(e_{35}+\frac{\partial e_{34}}{\partial\theta}\right)\frac{\partial}{r\partial z}+\left(\frac{\partial e_{24}}{\partial\theta}\right)\frac{\partial}{r^2\partial\theta}+(e_{25}+e_{14})\frac{\partial^2}{r\partial r\partial\theta}\\&\left.+\left(e_{34}+e_{23}\right)\frac{\partial^2}{r\partial\theta\partial z}+(e_{35}+e_{13})\frac{\partial^2}{\partial r\partial z}+e_{24}\frac{\partial^2}{r^2\partial\theta^2}\right]\phi=0,\end{aligned}\tag{7c}$$

$$\begin{aligned}&\left[e_{11}\frac{\partial^2}{\partial r^2}+e_{35}\frac{\partial^2}{\partial z^2}+\left(e_{11}+e_{12}+\frac{\partial e_{21}}{\partial\theta}\right)\frac{\partial}{r\partial r}+\left(e_{15}+e_{32}+\frac{\partial e_{25}}{\partial\theta}\right)\frac{\partial}{r\partial z}\right.\\&+\left(e_{22}+\frac{\partial e_{26}}{\partial\theta}\right)\frac{\partial}{r^2\partial\theta}+(e_{16}+e_{21})\frac{\partial^2}{r\partial r\partial\theta}+(e_{25}+e_{36})\frac{\partial^2}{r\partial\theta\partial z}\\&\left.+(e_{15}+e_{31})\frac{\partial^2}{\partial r\partial z}+\left(\frac{\partial e_{22}}{\partial\theta}+e_{26}\frac{\partial^2}{\partial\theta^2}\right)\frac{1}{r^2}\right]u_r+\left[e_{16}\frac{\partial^2}{\partial r^2}+e_{34}\frac{\partial^2}{\partial z^2}\right.\\&+\left(\frac{\partial e_{26}}{\partial\theta}\right)\frac{\partial}{r\partial r}+\left(e_{14}-e_{36}+\frac{\partial e_{24}}{\partial\theta}\right)\frac{\partial}{r\partial z}+\left(-e_{26}+\frac{\partial e_{22}}{\partial\theta}\right)\frac{\partial}{r^2\partial\theta}\\&+(e_{12}+e_{26})\frac{\partial^2}{r\partial r\partial\theta}+(e_{24}+e_{32})\frac{\partial^2}{r\partial\theta\partial z}+(e_{14}+e_{36})\frac{\partial^2}{\partial r\partial z}\\&\left.+\left(-\frac{\partial e_{26}}{\partial\theta}+e_{22}\frac{\partial^2}{\partial\theta^2}\right)\frac{1}{r^2}\right]u_\theta+\left[e_{15}\frac{\partial^2}{\partial r^2}+e_{33}\frac{\partial^2}{\partial z^2}+\left(e_{15}+\frac{\partial e_{25}}{\partial\theta}\right)\frac{\partial}{r\partial r}\right.\\&+\left(e_{13}+\frac{\partial e_{23}}{\partial\theta}\right)\frac{\partial}{r\partial z}+\left(\frac{\partial e_{24}}{\partial\theta}\right)\frac{\partial}{r^2\partial\theta}+(e_{14}+e_{25})\frac{\partial^2}{r\partial r\partial\theta}\\&\left.+(e_{23}+e_{34})\frac{\partial^2}{r\partial\theta\partial z}+(e_{13}+e_{35})\frac{\partial^2}{\partial r\partial z}+e_{24}\frac{\partial^2}{r^2\partial\theta^2}\right]u_z\\&-\left[\eta_{11}\frac{\partial^2}{\partial r^2}+\eta_{33}\frac{\partial^2}{\partial z^2}+\left(\eta_{11}+\frac{\partial\eta_{12}}{\partial\theta}\right)\frac{\partial}{r\partial r}+\left(\frac{\partial\eta_{22}}{\partial\theta}\right)\frac{\partial}{r^2\partial\theta}\right.\\&+\left(\eta_{13}+\frac{\partial\eta_{23}}{\partial\theta}\right)\frac{\partial}{r\partial z}+2\eta_{12}\frac{\partial^2}{r\partial r\partial\theta}+2\eta_{23}\frac{\partial^2}{r\partial\theta\partial z}\\&\left.+2\eta_{13}\frac{\partial^2}{\partial r\partial z}+\eta_{22}\frac{\partial^2}{r^2\partial\theta^2}\right]\phi=0.\end{aligned}\tag{7d}$$

Notably, the coefficients in the above partial differential equations are functions of θ and γ (Appendix A), and the assumption of axisymmetric deformation does not hold.

Fig. 2 shows a half plane with any constant θ in Fig. 1. To find an asymptotic solution around the sharp corner in Fig. 2, (r,Z) coordinates are transformed to (ρ,ϕ) coordinates as shown in Fig. 2. Transforming Eqs. (7) from (r,Z) to (ρ,ϕ) using the relations,

$$\rho=\sqrt{(r-R)^2+z^2},\quad \varphi=\tan^{-1}\left(\frac{-z}{r-R}\right),\quad r-R=\rho\cos\varphi,$$
$$\text{and}\quad z=-\rho\sin\varphi,\tag{8}$$

yields the following complicated partial differential equations with variable coefficients;

$$\begin{aligned}&\left\{(c_{11}L_1+c_{55}L_3+2c_{15}L_5)+\frac{1}{\rho\cos\varphi+R}\left[\left(c_{11}+\frac{\partial c_{16}}{\partial\theta}+2c_{16}\frac{\partial}{\partial\theta}\right)L_2\right.\right.\\&\left.+\left(c_{15}+\frac{\partial c_{56}}{\partial\theta}+2c_{56}\frac{\partial}{\partial\theta}\right)L_4\right]+\frac{1}{(\rho\cos\varphi+R)^2}\left[-c_{22}+\frac{\partial c_{26}}{\partial\theta}\right.\\&\left.\left.+c_{66}\frac{\partial^2}{\partial\theta^2}+\frac{\partial c_{66}}{\partial\theta}\frac{\partial}{\partial\theta}\right]\right\}u_r+\{(c_{16}L_1+c_{45}L_3+(c_{14}+c_{56})L_5)\\&+\frac{1}{\rho\cos\varphi+R}\left[\left(-c_{26}+\frac{\partial c_{66}}{\partial\theta}+(c_{12}+c_{66})\frac{\partial}{\partial\theta}\right)L_2\right.\\&\left.+\left(c_{14}-c_{24}-c_{56}+\frac{\partial c_{46}}{\partial\theta}+(c_{25}+c_{46})\frac{\partial}{\partial\theta}\right)L_4\right]\\&\left.+\frac{1}{(\rho\cos\varphi+R)^2}\left[c_{26}-\frac{\partial c_{66}}{\partial\theta}+\left(-c_{22}-c_{66}+\frac{\partial c_{26}}{\partial\theta}\right)\frac{\partial}{\partial\theta}+c_{26}\frac{\partial^2}{\partial\theta^2}\right]\right\}u_\theta\\&+\{(c_{15}L_1+c_{35}L_3+(c_{13}+c_{55})L_5)\\&+\frac{1}{\rho\cos\varphi+R}\left[\left(c_{15}-c_{25}+\frac{\partial c_{56}}{\partial\theta}+(c_{14}+c_{56})\frac{\partial}{\partial\theta}\right)L_2\right.\\&\left.+\left(c_{13}-c_{23}+\frac{\partial c_{36}}{\partial\theta}+(c_{36}+c_{45})\frac{\partial}{\partial\theta}\right)L_4\right]\\&\left.+\frac{1}{(\rho\cos\varphi+R)^2}\left[\left(-c_{24}+\frac{\partial c_{46}}{\partial\theta}\right)\frac{\partial}{\partial\theta}+c_{46}\frac{\partial^2}{\partial\theta^2}\right]\right\}u_z\\&+\{(e_{11}L_1+e_{35}L_3+(e_{31}+e_{15})L_5)\\&+\frac{1}{\rho\cos\varphi+R}\left[\left(e_{11}-e_{12}+\frac{\partial e_{16}}{\partial\theta}+(e_{16}+e_{21})\frac{\partial}{\partial\theta}\right)L_2\right.\\&\left.+\left(e_{31}-e_{32}+\frac{\partial e_{36}}{\partial\theta}+(e_{25}+e_{36})\frac{\partial}{\partial\theta}\right)L_4\right]\\&\left.+\frac{1}{(\rho\cos\varphi+R})^2\left[\left(-e_{22}+\frac{\partial e_{26}}{\partial\theta}\right)\frac{\partial}{\partial\theta}+e_{26}\frac{\partial^2}{\partial\theta^2}\right]\right\}\phi=0,\end{aligned}\tag{9a}$$

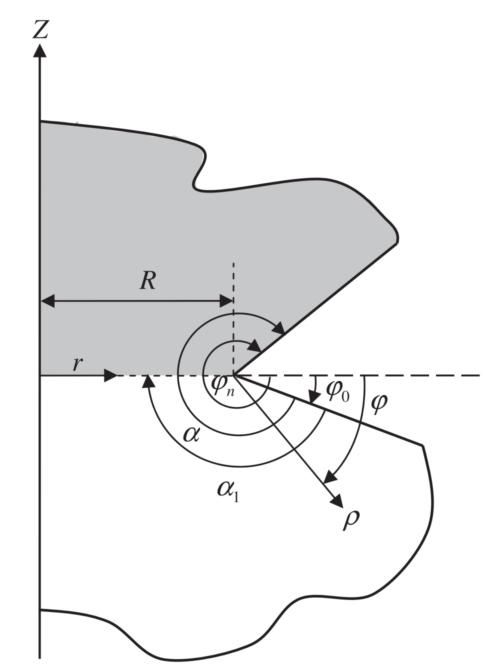

Fig. 2. Cylindrical (r, Z) and sharp corner (ρ,ϕ) coordinates.

$$
\begin{aligned}
&\{(c_{16}L_1+c_{45}L_3+(c_{56}+c_{14})L_5)\\
&\quad+\frac{1}{\rho\cos\varphi+R}\biggl[\biggl(2c_{16}+c_{26}+\frac{\partial c_{12}}{\partial\theta}+(c_{21}+c_{66})\frac{\partial}{\partial\theta}\biggr)L_2\\
&\quad+\biggl(2c_{56}+c_{24}+\frac{\partial c_{25}}{\partial\theta}+(c_{25}+c_{46})\frac{\partial}{\partial\theta}\biggr)L_4\biggr]\\
&\quad+\frac{1}{(\rho\cos\varphi+R)^2}\biggl(c_{26}+\frac{\partial c_{22}}{\partial\theta}+\biggl(c_{22}+c_{66}+\frac{\partial c_{26}}{\partial\theta}\biggr)\frac{\partial}{\partial\theta}+c_{26}\frac{\partial^2}{\partial\theta^2}\biggr)\biggr\}u_r\\
&\quad+\biggl\{(c_{66}L_1+c_{44}L_3+2c_{46}L_5)+\frac{1}{\rho\cos\varphi+R}\biggl[\biggl(c_{66}+\frac{\partial c_{26}}{\partial\theta}+2c_{26}\frac{\partial}{\partial\theta}\biggr)L_2\\
&\quad+\biggl(c_{46}+\frac{\partial c_{24}}{\partial\theta}+2c_{24}\frac{\partial}{\partial\theta}\biggr)L_4\biggr]+\frac{1}{(\rho\cos\varphi+R)^2}\biggl(-c_{66}-\frac{\partial c_{26}}{\partial\theta}\\
&\quad+\biggl(\frac{\partial c_{22}}{\partial\theta}\biggr)\frac{\partial}{\partial\theta}+c_{22}\frac{\partial^2}{\partial\theta^2}\biggr)\biggr\}u_\theta+\{(c_{56}L_1+c_{34}L_3+(c_{36}+c_{45})L_5)\\
&\quad+\frac{1}{\rho\cos\varphi+R}\biggl[\biggl(2c_{56}+\frac{\partial c_{25}}{\partial\theta}+(c_{25}+c_{46})\frac{\partial}{\partial\theta}\biggr)L_2\\
&\quad+\biggl(2c_{36}+\frac{\partial c_{23}}{\partial\theta}+(c_{23}+c_{44})\frac{\partial}{\partial\theta}\biggr)L_4\biggr]\\
&\quad+\frac{1}{(\rho\cos\varphi+R)^2}\biggl[\biggl(c_{46}+\frac{\partial c_{24}}{\partial\theta}\biggr)\frac{\partial}{\partial\theta}+c_{24}\frac{\partial^2}{\partial\theta^2}\biggr]\biggr\}u_z\\
&\quad+\{(e_{16}L_1+e_{34}L_3+(e_{36}+e_{14})L_5)\\
&\quad+\frac{1}{\rho\cos\varphi+R}\biggl[\biggl(2e_{16}+\frac{\partial e_{12}}{\partial\theta}+(e_{12}+e_{26})\frac{\partial}{\partial\theta}\biggr)\\
&\quad\times L_2\biggl(2e_{36}+\frac{\partial e_{32}}{\partial\theta}+(e_{24}+e_{32})\frac{\partial}{\partial\theta}\biggr)L_4\biggr]\\
&\quad+\frac{1}{(\rho\cos\varphi+R)^2}\biggl[\biggl(e_{26}+\frac{\partial e_{22}}{\partial\theta}\biggr)\frac{\partial}{\partial\theta}+e_{22}\frac{\partial^2}{\partial\theta^2}\biggr]\biggr\}\phi=0,
\end{aligned}
\tag{9b}
$$

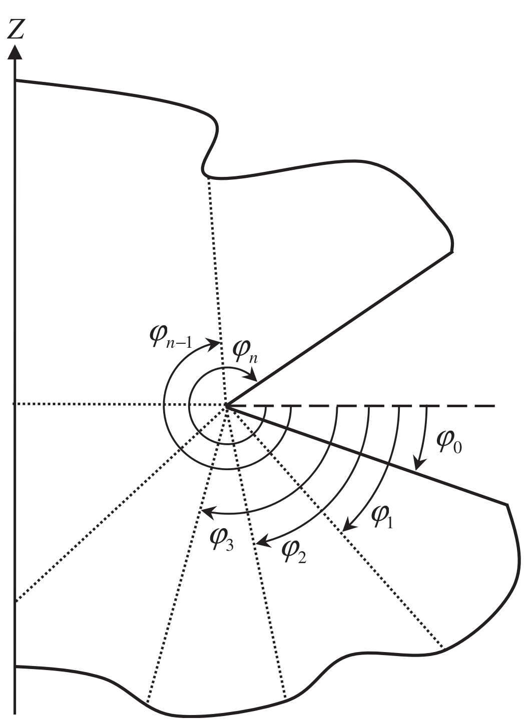

Fig. 3. Sub-domains for $\varphi\in[\varphi_0,\varphi_n]$.

$$
\begin{aligned}
&\{(c_{15}L_1+c_{35}L_3+(c_{55}+c_{13})L_5)\\
&\quad+\frac{1}{\rho\cos\varphi+R}\biggl[\biggl(c_{15}+c_{25}+\frac{\partial c_{14}}{\partial\theta}+(c_{14}+c_{56})\frac{\partial}{\partial\theta}\biggr)L_2\\
&\quad+\biggl(c_{23}+c_{55}+\frac{\partial c_{45}}{\partial\theta}+(c_{45}+c_{36})\frac{\partial}{\partial\theta}\biggr)L_4\biggr]\\
&\quad+\frac{1}{(\rho\cos\varphi+R)^2}\biggl(\frac{\partial c_{24}}{\partial\theta}+\biggl(c_{24}+\frac{\partial c_{46}}{\partial\theta}\biggr)\frac{\partial}{\partial\theta}+c_{46}\frac{\partial^2}{\partial\theta^2}\biggr)\biggr\}u_r\\
&\quad+\{(c_{56}L_1+c_{34}L_3+(c_{45}+c_{36})L_5)\\
&\quad+\frac{1}{\rho\cos\varphi+R}\biggl[\biggl(\frac{\partial c_{46}}{\partial\theta}+(c_{25}+c_{46})\frac{\partial}{\partial\theta}\biggr)L_2\\
&\quad+\biggl(c_{45}-c_{36}+\frac{\partial c_{44}}{\partial\theta}+(c_{44}+c_{23})\frac{\partial}{\partial\theta}\biggr)L_4\biggr]\\
&\quad+\frac{1}{(\rho\cos\varphi+R)^2}\biggl[-\frac{\partial c_{46}}{\partial\theta}+\biggl(-c_{46}+\frac{\partial c_{24}}{\partial\theta}\biggr)\frac{\partial}{\partial\theta}+c_{24}\frac{\partial^2}{\partial\theta^2}\biggr]\biggr\}u_\theta\\
&\quad+\biggl\{(c_{55}L_1+c_{33}L_3+2c_{35}L_5)+\frac{1}{\rho\cos\varphi+R}\\
&\quad\times\biggl[\biggl(c_{55}+\frac{\partial c_{45}}{\partial\theta}+2c_{45}\frac{\partial}{\partial\theta}\biggr)L_2+\biggl(c_{35}+\frac{\partial c_{34}}{\partial\theta}+2c_{34}\frac{\partial}{\partial\theta}\biggr)L_4\biggr]\\
&\quad+\frac{1}{(\rho\cos\varphi+R)^2}\biggl(\biggl(\frac{\partial c_{44}}{\partial\theta}\biggr)\frac{\partial}{\partial\theta}+c_{44}\frac{\partial^2}{\partial\theta^2}\biggr)\biggr\}u_z\\
&\quad+\{(e_{15}L_1+e_{33}L_3+(e_{35}+e_{13})L_5)\\
&\quad+\frac{1}{\rho\cos\varphi+R}\biggl[\biggl(e_{15}+\frac{\partial e_{14}}{\partial\theta}+(e_{25}+e_{14})\frac{\partial}{\partial\theta}\biggr)L_2\\
&\quad+\biggl(e_{35}+\frac{\partial e_{34}}{\partial\theta}+(e_{34}+e_{23})\frac{\partial}{\partial\theta}\biggr)L_4\biggr]\\
&\quad+\frac{1}{(\rho\cos\varphi+R})^2\biggl[\biggl(\frac{\partial e_{24}}{\partial\theta}\biggr)\frac{\partial}{\partial\theta}+e_{24}\frac{\partial^2}{\partial\theta^2}\biggr]\biggr\}\phi=0,
\end{aligned}
\tag{9c}
$$

$$
\begin{aligned}
&\{(e_{11}L_1+e_{35}L_3+(e_{15}+e_{31})L_5)\\
&\quad+\frac{1}{\rho\cos\varphi+R}\biggl[\biggl(e_{11}+e_{12}+\frac{\partial e_{21}}{\partial\theta}+(e_{16}+e_{21})\frac{\partial}{\partial\theta}\biggr)L_2\\
&\quad+\biggl(e_{15}+e_{32}+\frac{\partial e_{25}}{\partial\theta}+(e_{25}+e_{36})\frac{\partial}{\partial\theta}\biggr)L_4\biggr]\\
&\quad+\frac{1}{(\rho\cos\varphi+R)^2}\biggl(\frac{\partial e_{22}}{\partial\theta}+\biggl(e_{22}+\frac{\partial e_{26}}{\partial\theta}\biggr)\frac{\partial}{\partial\theta}+e_{26}\frac{\partial^2}{\partial\theta^2}\biggr)\biggr\}u_r\\
&\quad+\{(e_{16}L_1+e_{34}L_3+(e_{14}+e_{36})L_5)\\
&\quad+\frac{1}{\rho\cos\varphi+R}\biggl[\biggl(\frac{\partial e_{26}}{\partial\theta}+(e_{12}+e_{26})\frac{\partial}{\partial\theta}\biggr)L_2\\
&\quad+\biggl(e_{14}-e_{36}+\frac{\partial e_{24}}{\partial\theta}+(e_{24}+e_{32})\frac{\partial}{\partial\theta}\biggr)L_4\biggr]\\
&\quad+\frac{1}{(\rho\cos\varphi+R)^2}\biggl[-\frac{\partial e_{26}}{\partial\theta}+\biggl(-e_{26}+\frac{\partial e_{22}}{\partial\theta}\biggr)\frac{\partial}{\partial\theta}+e_{22}\frac{\partial^2}{\partial\theta^2}\biggr]\biggr\}u_\theta\\
&\quad+\{(e_{15}L_1+e_{33}L_3+(e_{13}+e_{35})L_5)\\
&\quad+\frac{1}{\rho\cos\varphi+R}\biggl[\biggl(e_{15}+\frac{\partial e_{25}}{\partial\theta}+(e_{14}+e_{25})\frac{\partial}{\partial\theta}\biggr)L_2\\
&\quad+\biggl(e_{13}+\frac{\partial e_{23}}{\partial\theta}+(e_{23}+e_{34})\frac{\partial}{\partial\theta}\biggr)L_4\biggr]\\
&\quad+\frac{1}{(\rho\cos\varphi+R})^2\biggl[\biggl(\frac{\partial e_{24}}{\partial\theta}\biggr)\frac{\partial}{\partial\theta}+e_{24}\frac{\partial^2}{\partial\theta^2}\biggr]\biggr\}u_z\\
&\quad-\biggl\{(\eta_{11}L_1+\eta_{33}L_3+2\eta_{13}L_5)+\frac{1}{\rho\cos\varphi+R}\\
&\quad\times\biggl[\biggl(\eta_{11}+\frac{\partial\eta_{12}}{\partial\theta}+2\eta_{12}\frac{\partial}{\partial\theta}\biggr)L_2+\biggl(\eta_{13}+\frac{\partial\eta_{23}}{\partial\theta}+2\eta_{23}\frac{\partial}{\partial\theta}\biggr)L_4\biggr]\\
&\quad+\frac{1}{(\rho\cos\varphi+R)^2}\biggl[\biggl(\frac{\partial\eta_{22}}{\partial\theta}\biggr)\frac{\partial}{\partial\theta}+\eta_{22}\frac{\partial^2}{\partial\theta^2}\biggr]\biggr\}\phi=0,
\end{aligned}
\tag{9d}
$$

where

$$L_1=\cos^2\varphi\frac{\partial^2}{\partial\rho^2}+\frac{\sin^2\varphi}{\rho}\frac{\partial}{\partial\rho}-\frac{2\sin\varphi\cos\varphi}{\rho}\frac{\partial^2}{\partial\rho\partial\varphi}+\frac{2\sin\varphi\cos\varphi}{\rho^2}\frac{\partial}{\partial\varphi}+\frac{\sin^2\varphi}{\rho^2}\frac{\partial^2}{\partial\varphi^2},$$
$$L_2=\cos\varphi\frac{\partial}{\partial\rho}-\frac{\sin\varphi}{\rho}\frac{\partial}{\partial\varphi},$$
$$L_3=\sin^2\varphi\frac{\partial^2}{\partial\rho^2}+\frac{\cos^2\varphi}{\rho}\frac{\partial}{\partial\rho}+\frac{2\sin\varphi\cos\varphi}{\rho}\frac{\partial^2}{\partial\rho\partial\varphi}-\frac{2\sin\varphi\cos\varphi}{\rho^2}\frac{\partial}{\partial\varphi}+\frac{\cos^2\varphi}{\rho^2}\frac{\partial^2}{\partial\varphi^2},$$
$$L_4=\frac{\partial}{\partial\rho}\frac{\partial\rho}{\partial z}+\frac{\partial}{\partial\varphi}\frac{\partial\varphi}{\partial z}=-\sin\varphi\frac{\partial}{\partial\rho}-\frac{\cos\varphi}{\rho}\frac{\partial}{\partial\varphi},$$
$$L_5=-\sin\varphi\cos\varphi\frac{\partial^2}{\partial\rho^2}+\frac{\sin\varphi\cos\varphi}{\rho}\frac{\partial}{\partial\rho}-\frac{\cos2\varphi}{\rho}\frac{\partial^2}{\partial\rho\partial\varphi}+\frac{\cos2\varphi}{\rho^2}\frac{\partial}{\partial\varphi}+\frac{\sin\varphi\cos\varphi}{\rho^2}\frac{\partial^2}{\partial\varphi^2},$$

3. Asymptotic solution at a sharp corner

To find solutions to Eqs. (9) for bodies of revolution, the methodology of Hartranft and Sih [3] for elastic wedges can be applied. The solutions are expressed as

$$u_r(r,\theta,z)=\sum_{m=0}^{\infty}\sum_{n=0}^{\infty}\rho^{\lambda_m+n}\widehat{U}_n^{(m)}(\theta,\varphi),$$
$$u_\theta(r,\theta,z)=\sum_{m=0}^{\infty}\sum_{n=0}^{\infty}\rho^{\lambda_m+n}\widehat{V}_n^{(m)}(\theta,\varphi),$$
$$u_z(r,\theta,z)=\sum_{m=0}^{\infty}\sum_{n=0}^{\infty}\rho^{\lambda_m+n}\widehat{W}_n^{(m)}(\theta,\varphi),$$
$$\phi(r,\theta,z)=\sum_{m=0}^{\infty}\sum_{n=0}^{\infty}\rho^{\lambda_m+n}\widehat{\Phi}_n^{(m)}(\theta,\varphi),\tag{10}$$

where λ_m is a parameter to be determined, which can be a complex number, and the real part of λ_m must be positive to ensure finite displacement and electric potential at $\rho = 0$. To determine the eletro-elastic singularity behaviors as ρ approaches zero, substituting Eq. 10 into Eqs. (9) with careful arrangement and considering only the equations for the least power order of ρ yield

$$\begin{aligned}
&\frac{\partial^2\widehat{U}_0^{(m)}}{\partial\varphi^2}+\frac{1}{\Delta_1}(\lambda_m-1)[(c_{55}-c_{11})\sin2\varphi-2c_{15}\cos2\varphi]\frac{\partial\widehat{U}_0^{(m)}}{\partial\varphi}\\
&+\frac{1}{\Delta_1}\Big[\lambda_m((\lambda_m-1)c_{55}+c_{11})\sin^2\varphi+\lambda_m((\lambda_m-1)c_{11}+c_{55})\cos^2\varphi\\
&+\lambda_m(2-\lambda_m)c_{15}\sin2\varphi\Big]\widehat{U}_0^{(m)}+\frac{1}{\Delta_1}\Big\{\Big[c_{16}\sin^2\varphi+c_{45}\cos^2\varphi\\
&+\frac{(c_{14}+c_{56})}{2}\sin2\varphi\Big]\frac{\partial^2\widehat{V}_0^{(m)}}{\partial\varphi^2}+(\lambda_m-1)[(c_{45}-c_{16})\sin2\varphi\\
&-(c_{14}+c_{56})\cos2\varphi]\frac{\partial\widehat{V}_0^{(m)}}{\partial\varphi}+\Big[\lambda_m(\lambda_m-1)\big(c_{16}\cos^2\varphi\\
&+c_{45}\sin^2\varphi-\frac{(c_{14}+c_{56})}{2}\sin2\varphi\Big)+\lambda_m\Big(c_{16}\sin^2\varphi+c_{45}\cos^2\varphi\\
&+\frac{(c_{14}+c_{56})}{2}\sin2\varphi\Big)\Big]\Big\}\widehat{V}_0^{(m)}+\frac{1}{\Delta_1}\Big\{\Big[c_{15}\sin^2\varphi+c_{35}\cos^2\varphi\\
&+\frac{(c_{13}+c_{55})}{2}\sin2\varphi\Big]\frac{\partial^2\widehat{W}_0^{(m)}}{\partial\varphi^2}+(\lambda_m-1)[(c_{35}-c_{15})\sin2\varphi\\
&-(c_{13}+c_{55})\cos2\varphi]\frac{\partial\widehat{W}_0^{(m)}}{\partial\varphi}+\Big[\lambda_m(\lambda_m-1)\Big(c_{15}\cos^2\varphi+c_{35}\sin^2\varphi\\
&-\frac{(c_{13}+c_{55})}{2}\sin2\varphi\Big)+\lambda_m\Big(c_{15}\sin^2\varphi+c_{35}\cos^2\varphi\\
&+\frac{(c_{13}+c_{55})}{2}\sin2\varphi\Big)\Big]\Big\}\widehat{W}_0^{(m)}+\frac{1}{\Delta_1}\Big\{\Big[e_{11}\sin^2\varphi+e_{35}\cos^2\varphi\\
&+\frac{(e_{15}+e_{31})}{2}\sin2\varphi\Big]\frac{\partial^2\widehat{\Phi}_0^{(m)}}{\partial\varphi^2}+(\lambda_m-1)[(e_{35}-e_{15})\sin2\varphi\\
&-(e_{15}+e_{31})\cos2\varphi]\frac{\partial\widehat{\Phi}_0^{(m)}}{\partial\varphi}+\Big[\lambda_m(\lambda_m-1)\Big(e_{11}\cos^2\varphi+e_{35}\sin^2\varphi\\
&-\frac{(e_{15}+e_{31})}{2}\sin2\varphi\Big)+\lambda_m\Big(e_{11}\sin^2\varphi+e_{35}\cos^2\varphi\\
&+\frac{(e_{15}+e_{31})}{2}\sin2\varphi\Big)\Big]\Big\}\widehat{\Phi}_0^{(m)}=0,
\end{aligned}\tag{11a}$$

$$\begin{aligned}
&\frac{\partial^2\widehat{V}_0^{(m)}}{\partial\varphi^2}+\frac{1}{\Delta_2}(\lambda_m-1)[(c_{44}-c_{66})\sin2\varphi-2c_{46}\cos2\varphi]\frac{\partial\widehat{V}_0^{(m)}}{\partial\varphi}\\
&+\frac{1}{\Delta_2}\Big[\lambda_m((\lambda_m-1)c_{44}+c_{66})\sin^2\varphi+\lambda_m((\lambda_m-1)c_{66}+c_{44})\cos^2\varphi\\
&+\lambda_m(2-\lambda_m)c_{46}\sin2\varphi\Big]\widehat{V}_0^{(m)}+\frac{1}{\Delta_2}\Big\{\Big[c_{16}\sin^2\varphi+c_{45}\cos^2\varphi\\
&+\frac{(c_{56}+c_{14})}{2}\sin2\varphi\Big]\frac{\partial^2\widehat{U}_0^{(m)}}{\partial\varphi^2}+(\lambda_m-1)[(c_{45}-c_{16})\sin2\varphi\\
&-(c_{56}+c_{14})\cos2\varphi]\frac{\partial\widehat{U}_0^{(m)}}{\partial\varphi}+\Big[\lambda_m(\lambda_m-1)\Big(c_{16}\cos^2\varphi+c_{45}\sin^2\varphi\\
&-\frac{(c_{56}+c_{14})}{2}\sin2\varphi\Big)+\lambda_m\Big(c_{16}\sin^2\varphi+c_{45}\cos^2\varphi\\
&+\frac{(c_{56}+c_{14})}{2}\sin2\varphi\Big)\Big]\Big\}\widehat{U}_0^{(m)}+\frac{1}{\Delta_2}\Big\{\Big[c_{56}\sin^2\varphi+c_{34}\cos^2\varphi\\
&+\frac{(c_{36}+c_{45})}{2}\sin2\varphi\Big]\frac{\partial^2\widehat{W}_0^{(m)}}{\partial\varphi^2}+(\lambda_m-1)[(c_{34}-c_{56})\sin2\varphi\\
&-(c_{36}+c_{45})\cos2\varphi]\frac{\partial\widehat{W}_0^{(m)}}{\partial\varphi}+\Big[\lambda_m(\lambda_m-1)\Big(c_{56}\cos^2\varphi+c_{34}\sin^2\varphi\\
&-\frac{(c_{36}+c_{45})}{2}\sin2\varphi\Big)+\lambda_m\Big(c_{56}\sin^2\varphi+c_{34}\cos^2\varphi\\
&+\frac{(c_{36}+c_{45})}{2}\sin2\varphi\Big)\Big]\Big\}\widehat{W}_0^{(m)}+\frac{1}{\Delta_2}\Big\{\Big[e_{16}\sin^2\varphi+e_{34}\cos^2\varphi\\
&+\frac{(e_{36}+e_{14})}{2}\sin2\varphi\Big]\frac{\partial^2\widehat{\Phi}_0^{(m)}}{\partial\varphi^2}+(\lambda_m-1)[(e_{34}-e_{16})\sin2\varphi\\
&-(e_{36}+e_{14})\cos2\varphi]\frac{\partial\widehat{\Phi}_0^{(m)}}{\partial\varphi}+\Big[\lambda_m(\lambda_m-1)\Big(e_{16}\cos^2\varphi+e_{34}\sin^2\varphi\\
&-\frac{(e_{36}+e_{14})}{2}\sin2\varphi\Big)+\lambda_m\Big(e_{16}\sin^2\varphi+e_{34}\cos^2\varphi\\
&+\frac{(e_{36}+e_{14})}{2}\sin2\varphi\Big)\Big]\Big\}\widehat{\Phi}_0^{(m)}=0,
\end{aligned}\tag{11b}$$

$$\begin{aligned}
&\frac{\partial^2\widehat{W}_0^{(m)}}{\partial\varphi^2}+\frac{1}{\Delta_3}(\lambda_m-1)[(c_{33}-c_{55})\sin2\varphi-2c_{35}\cos2\varphi]\frac{\partial\widehat{W}_0^{(m)}}{\partial\varphi}\\
&+\frac{1}{\Delta_3}\Big[\lambda_m((\lambda_m-1)c_{33}+c_{55})\sin^2\varphi+\lambda_m((\lambda_m-1)c_{55}+c_{33})\cos^2\varphi\\
&+\lambda_m(2-\lambda_m)c_{35}\sin2\varphi\Big]\widehat{W}_0^{(m)}+\frac{1}{\Delta_3}\Big\{\Big[c_{15}\sin^2\varphi+c_{35}\cos^2\varphi\\
&+\frac{(c_{31}+c_{55})}{2}\sin2\varphi\Big]\frac{\partial^2\widehat{U}_0^{(m)}}{\partial\varphi^2}+(\lambda_m-1)[(c_{35}-c_{15})\sin2\varphi
\end{aligned}$$

$$- (c_{13}+c_{55})\cos 2\varphi]\frac{\partial \widehat{U}_0^{(m)}}{\partial\varphi} + \Big[\lambda_m(\lambda_m-1)(c_{15}\cos^2\varphi + c_{35}\sin^2\varphi - \frac{(c_{13}+c_{55})}{2}\sin 2\varphi) + \lambda_m\Big(c_{15}\sin^2\varphi + c_{35}\cos^2\varphi + \frac{(c_{13}+c_{55})}{2}\sin 2\varphi\Big)\Big]\Big\}\widehat{U}_0^{(m)} + \frac{1}{\Delta_3}\Big\{\Big[c_{56}\sin^2\varphi + c_{34}\cos^2\varphi + \frac{(c_{36}+c_{45})}{2}\sin 2\varphi\Big]\frac{\partial^2\widehat{V}_0^{(m)}}{\partial\varphi^2} + (\lambda_m-1)[(c_{34}-c_{56})\sin 2\varphi - (c_{36}+c_{45})\cos 2\varphi]\frac{\partial\widehat{V}_0^{(m)}}{\partial\varphi} + \Big[\lambda_m(\lambda_m-1)\Big(c_{56}\cos^2\varphi + c_{34}\sin^2\varphi - \frac{(c_{36}+c_{45})}{2}\sin 2\varphi\Big) + \lambda_m\Big(c_{56}\sin^2\varphi + c_{34}\cos^2\varphi + \frac{(c_{36}+c_{45})}{2}\sin 2\varphi\Big)\Big]\Big\}\widehat{V}_0^{(m)} + \frac{1}{\Delta_3}\Big\{\Big[e_{15}\sin^2\varphi + e_{33}\cos^2\varphi + \frac{(e_{13}+e_{35})}{2}\sin 2\varphi\Big]\frac{\partial^2\widehat{\Phi}_0^{(m)}}{\partial\varphi^2} + (\lambda_m-1)[(e_{33}-e_{15})\sin 2\varphi - (e_{13}+e_{35})\cos 2\varphi]\frac{\partial\widehat{\Phi}_0^{(m)}}{\partial\varphi} + \Big[\lambda_m(\lambda_m-1)\Big(e_{15}\cos^2\varphi + e_{33}\sin^2\varphi - \frac{(e_{13}+e_{35})}{2}\sin 2\varphi\Big) + \lambda_m\Big(e_{15}\sin^2\varphi + e_{33}\cos^2\varphi + \frac{(e_{13}+e_{35})}{2}\sin 2\varphi\Big)\Big]\Big\}\widehat{\Phi}_0^{(m)} = 0, \tag{11c}$$

$$\frac{\partial^2\widehat{\Phi}_0^{(m)}}{\partial\varphi^2} + \frac{1}{\Delta_4}(\lambda_m-1)[(\eta_{33}-\eta_{11})\sin 2\varphi - 2\eta_{13}\cos 2\varphi]\frac{\partial\widehat{\Phi}_0^{(m)}}{\partial\varphi} + \frac{1}{\Delta_4}\Big[\lambda_m((\lambda_m-1)\eta_{33}+\eta_{11})\sin^2\varphi + \lambda_m((\lambda_m-1)\eta_{11}+\eta_{33})\cos^2\varphi + \lambda_m(2-\lambda_m)\eta_{13}\sin 2\varphi\Big]\widehat{\Phi}_0^{(m)} - \frac{1}{\Delta_4}\Big\{\Big[e_{11}\sin^2\varphi + e_{35}\cos^2\varphi + \frac{(e_{15}+e_{31})}{2}\sin 2\varphi\Big]\frac{\partial^2\widehat{U}_0^{(m)}}{\partial\varphi^2} + (\lambda_m-1)[(e_{35}-e_{11})\sin 2\varphi - (e_{15}+e_{31})\cos 2\varphi]\frac{\partial\widehat{U}_0^{(m)}}{\partial\varphi} + \Big[\lambda_m(\lambda_m-1)\Big(e_{11}\cos^2\varphi + e_{35}\sin^2\varphi - \frac{(e_{15}+e_{31})}{2}\sin 2\varphi\Big) + \lambda_m\Big(e_{11}\sin^2\varphi + e_{35}\cos^2\varphi + \frac{(e_{15}+e_{31})}{2}\sin 2\varphi\Big)\Big]\Big\}\widehat{U}_0^{(m)} - \frac{1}{\Delta_4}\Big\{\Big[e_{16}\sin^2\varphi + e_{34}\cos^2\varphi + \frac{(e_{14}+e_{36})}{2}\sin 2\varphi\Big]\frac{\partial^2\widehat{V}_0^{(m)}}{\partial\varphi^2} + (\lambda_m-1)[(e_{34}-e_{16})\sin 2\varphi - (e_{14}+e_{36})\cos 2\varphi]\frac{\partial\widehat{V}_0^{(m)}}{\partial\varphi} + \Big[\lambda_m(\lambda_m-1)\Big(e_{16}\cos^2\varphi + e_{34}\sin^2\varphi - \frac{(e_{14}+e_{36})}{2}\sin 2\varphi\Big) + \lambda_m\Big(e_{16}\sin^2\varphi + e_{34}\cos^2\varphi + \frac{(e_{14}+e_{36})}{2}\sin 2\varphi\Big)\Big]\Big\}\widehat{V}_0^{(m)} - \frac{1}{\Delta_4}\Big\{\Big[e_{15}\sin^2\varphi + e_{33}\cos^2\varphi + \frac{(e_{13}+e_{35})}{2}\sin 2\varphi\Big]\frac{\partial^2\widehat{W}_0^{(m)}}{\partial\varphi^2} + (\lambda_m-1)[(e_{33}-e_{15})\sin 2\varphi - (e_{13}+e_{35})\cos 2\varphi]\frac{\partial\widehat{W}_0^{(m)}}{\partial\varphi} + \Big[\lambda_m(\lambda_m-1)\Big(e_{15}\cos^2\varphi + e_{33}\sin^2\varphi - \frac{(e_{13}+e_{35})}{2}\sin 2\varphi\Big) + \lambda_m\Big(e_{15}\sin^2\varphi + e_{33}\cos^2\varphi + \frac{(e_{13}+e_{35})}{2}\sin 2\varphi\Big)\Big]\Big\}\widehat{W}_0^{(m)} = 0, \tag{11d}$$

where

$$\Delta_1 = c_{11}\sin^2\varphi + c_{55}\cos^2\varphi + c_{15}\sin 2\varphi,\quad \Delta_2 = c_{66}\sin^2\varphi + c_{44}\cos^2\varphi + c_{46}\sin 2\varphi,$$
$$\Delta_3 = c_{55}\sin^2\varphi + c_{33}\cos^2\varphi + c_{35}\sin 2\varphi,\quad \Delta_4 = \eta_{11}\sin^2\varphi + \eta_{33}\cos^2\varphi + \eta_{13}\sin 2\varphi.$$

Eqs. (11) are a set of ordinary differential equations with variable coefficients that are functions of φ, θ and γ. Finding a closed-form solution for these equations is generally impossible.

The power series method is utilized to find a general solution for Eqs. (11). Very high-order terms are typically required to obtain an accurate solution and can cause numerical difficulties. To overcome these difficulties, the range of φ under consideration is divided into a number of sub-domains (see Fig. 3). A series solution for Eqs. (11) is established in each sub-domain. Then, a general solution for the whole domain of φ is constructed from these series solutions in the sub-domains by satisfying the continuity conditions between each pair of adjacent sub-domains. This means of constructing solutions is very convenient for analyzing the bi-material body that is considered in this work.

With fixed θ and γ, the following functions that specify the variable coefficients in Eqs. (11) are expressed as Taylor expansions over sub-domain i;

$$\frac{\sin 2\varphi}{\Delta_1} = \sum_{k=0}^{K} a_k^{(i)}(\varphi-\bar{\varphi}_i)^k,\quad \frac{\cos^2\varphi}{\Delta_1} = \sum_{k=0}^{K} b_k^{(i)}(\varphi-\bar{\varphi}_i)^k,$$
$$\frac{\sin^2\varphi}{\Delta_1} = \sum_{k=0}^{K} c_k^{(i)}(\varphi-\bar{\varphi}_i)^k,\quad \frac{\cos 2\varphi}{\Delta_1} = \sum_{k=0}^{K} d_k^{(i)}(\varphi-\bar{\varphi}_i)^k,$$
$$\frac{\sin 2\varphi}{\Delta_2} = \sum_{k=0}^{K} e_k^{(i)}(\varphi-\bar{\varphi}_i)^k,\quad \frac{\cos^2\varphi}{\Delta_2} = \sum_{k=0}^{K} f_k^{(i)}(\varphi-\bar{\varphi}_i)^k,$$
$$\frac{\sin^2\varphi}{\Delta_2} = \sum_{k=0}^{K} g_k^{(i)}(\varphi-\bar{\varphi}_i)^k,\quad \frac{\cos 2\varphi}{\Delta_2} = \sum_{k=0}^{K} h_k^{(i)}(\varphi-\bar{\varphi}_i)^k,$$
$$\frac{\sin 2\varphi}{\Delta_3} = \sum_{k=0}^{K} l_k^{(i)}(\varphi-\bar{\varphi}_i)^k,\quad \frac{\cos^2\varphi}{\Delta_3} = \sum_{k=0}^{K} m_k^{(i)}(\varphi-\bar{\varphi}_i)^k,$$
$$\frac{\sin^2\varphi}{\Delta_3} = \sum_{k=0}^{K} n_k^{(i)}(\varphi-\bar{\varphi}_i)^k,\quad \frac{\cos 2\varphi}{\Delta_3} = \sum_{k=0}^{K} o_k^{(i)}(\varphi-\bar{\varphi}_i)^k,$$
$$\frac{\sin 2\varphi}{\Delta_4} = \sum_{k=0}^{K} p_k^{(i)}(\varphi-\bar{\varphi}_i)^k,\quad \frac{\cos^2\varphi}{\Delta_4} = \sum_{k=0}^{K} q_k^{(i)}(\varphi-\bar{\varphi}_i)^k,$$
$$\frac{\sin^2\varphi}{\Delta_4} = \sum_{k=0}^{K} r_k^{(i)}(\varphi-\bar{\varphi}_i)^k,\quad \frac{\cos 2\varphi}{\Delta_4} = \sum_{k=0}^{K} s_k^{(i)}(\varphi-\bar{\varphi}_i)^k, \tag{12}$$

where $\bar{\varphi}_i$ is a reference point in sub-domain i. Here, $\bar{\varphi}_i$ is chosen as the middle point along the φ in the sub-domain i. Consequently, the general solutions of Eqs. (11) in sub-domain i are expressed in the following form:

$$\widehat{U}_{0i}^{(m)} = \sum_{j=0}^{J}\widehat{A}_j^{(i)}(\varphi-\bar{\varphi}_i)^j,\quad \widehat{V}_{0i}^{(m)} = \sum_{j=0}^{J}\widehat{B}_j^{(i)}(\varphi-\bar{\varphi}_i)^j,$$
$$\widehat{W}_{0i}^{(m)} = \sum_{j=0}^{J}\widehat{C}_j^{(i)}(\varphi-\bar{\varphi}_i)^j,\quad \widehat{\Phi}_{0i}^{(m)} = \sum_{j=0}^{J}\widehat{D}_j^{(i)}(\varphi-\bar{\varphi}_i)^j. \tag{13}$$

Substituting Eq. (13) into Eqs. (11) with careful arrangement yields the recursive equations for the coefficients in Eq. (13),

$$
\begin{aligned}
&\widehat{A}^{(i)}_{j+2} + \left(c_{16}c^{(i)}_0 + c_{45}b^{(i)}_0 + \frac{(c_{14}+c_{56})}{2}a^{(i)}_0\right)\widehat{B}^{(i)}_{j+2} \\
&\quad + \left(c_{15}c^{(i)}_0 + c_{35}b^{(i)}_0 + \frac{(c_{13}+c_{55})}{2}a^{(i)}_0\right)\widehat{C}^{(i)}_{j+2} \\
&\quad + \left(e_{11}c^{(i)}_0 + e_{35}b^{(i)}_0 + \frac{(e_{15}+e_{31})}{2}a^{(i)}_0\right)\widehat{D}^{(i)}_{j+2} \\
&= \frac{-1}{(j+2)(j+1)}\Bigg\{\sum_{k=0}^{j-1}\Bigg[\Bigg(c_{16}c^{(i)}_{j-k} + c_{45}b^{(i)}_{j-k} + \frac{(c_{14}+c_{56})}{2}a^{(i)}_{j-k}\Bigg)\Bigg] \\
&\quad \times (k+2)(k+1)\widehat{B}^{(i)}_{k+2} + \left(c_{15}c^{(i)}_{j-k} + c_{35}b^{(i)}_{j-k} + \frac{(c_{13}+c_{55})}{2}a^{(i)}_{j-k}\right) \\
&\quad \times (k+2)(k+1)\widehat{C}^{(i)}_{k+2} + \left(e_{11}c^{(i)}_{j-k} + e_{35}b^{(i)}_{j-k} + \frac{(e_{15}+e_{31})}{2}a^{(i)}_{j-k}\right) \\
&\quad \times (k+2)(k+1)\widehat{D}^{(i)}_{k+2} + \sum_{k=0}^{j}\Big[(\lambda_m-1)\Big[(c_{55}-c_{11})a^{(i)}_{j-k} - 2c_{15}d^{(i)}_{j-k}\Big] \\
&\quad \times (k+1)\widehat{A}^{(i)}_{k+1} + \Big[\lambda_m((\lambda_m-1)c_{55}+c_{11})c^{(i)}_{j-k} + \lambda_m((\lambda_m-1)c_{11}+c_{55}) \\
&\quad \times b^{(i)}_{j-k} + \lambda_m(2-\lambda_m)c_{15}a^{(i)}_{j-k}\Big]\widehat{A}^{(i)}_k + (\lambda_m-1)\Big[(c_{45}-c_{16})a^{(i)}_{j-k} \\
&\quad - (c_{14}+c_{56})d^{(i)}_{j-k}\Big](k+1)\widehat{B}^{(i)}_{k+1} + \Big[\lambda_m(\lambda_m-1)\times\Big(c_{16}b^{(i)}_{j-k} + c_{45}c^{(i)}_{j-k} \\
&\quad - \frac{(c_{14}+c_{56})}{2}a^{(i)}_{j-k}\Big) + \lambda_m\left(c_{16}c^{(i)}_{j-k} + c_{45}b^{(i)}_{j-k} + \frac{(c_{14}+c_{56})}{2}a^{(i)}_{j-k}\right)\Big]\widehat{B}^{(i)}_k \\
&\quad + (\lambda_m-1)\Big[(c_{35}-c_{15})a^{(i)}_{j-k} - (c_{13}+c_{55})d^{(i)}_{j-k}\Big](k+1)\widehat{C}^{(i)}_{k+1} \\
&\quad + \Big[\lambda_m(\lambda_m-1)\left(c_{15}b^{(i)}_{j-k} + c_{35}c^{(i)}_{j-k} - \frac{(c_{13}+c_{55})}{2}a^{(i)}_{j-k}\right) \\
&\quad + \lambda_m\left(c_{15}c^{(i)}_{j-k} + c_{35}b^{(i)}_{j-k} + \frac{(c_{13}+c_{55})}{2}a^{(i)}_{j-k}\right)\Big]\widehat{C}^{(i)}_k \\
&\quad + (\lambda_m-1)\Big[(e_{35}-e_{11})a^{(i)}_{j-k} - (e_{15}+e_{31})d^{(i)}_{j-k}\Big](k+1)\widehat{D}^{(i)}_{k+1} \\
&\quad + \Big[\lambda_m(\lambda_m-1)\left(e_{11}b^{(i)}_{j-k} + e_{35}c^{(i)}_{j-k} - \frac{(e_{15}+e_{31})}{2}a^{(i)}_{j-k}\right) \\
&\quad + \lambda_m\left(e_{11}c^{(i)}_{j-k} + e_{35}b^{(i)}_{j-k} + \frac{(e_{15}+e_{31})}{2}a^{(i)}_{j-k}\right)\Big]\widehat{D}^{(i)}_k\Big]\Bigg\},
\end{aligned}
\tag{14a}
$$

$$
\begin{aligned}
&\widehat{B}^{(i)}_{j+2} + \left(c_{16}g^{(i)}_0 + c_{45}f^{(i)}_0 + \frac{(c_{56}+c_{14})}{2}e^{(i)}_0\right)\widehat{A}^{(i)}_{j+2} \\
&\quad + \left(c_{56}g^{(i)}_0 + c_{34}f^{(i)}_0 + \frac{(c_{36}+c_{45})}{2}e^{(i)}_0\right)\widehat{C}^{(i)}_{j+2} \\
&\quad + \left(e_{16}g^{(i)}_0 + e_{34}f^{(i)}_0 + \frac{(e_{36}+e_{14})}{2}e^{(i)}_0\right)\widehat{D}^{(i)}_{j+2} \\
&= \frac{-1}{(j+2)(j+1)}\Bigg\{\sum_{k=0}^{j-1}\Bigg[\Bigg(c_{16}g^{(i)}_{j-k} + c_{45}f^{(i)}_{j-k} + \frac{(c_{56}+c_{14})}{2}e^{(i)}_{j-k}\Bigg)\Bigg] \\
&\quad \times (k+2)(k+1)\widehat{A}^{(i)}_{k+2} + \left(c_{56}g^{(i)}_{j-k} + c_{34}f^{(i)}_{j-k} + \frac{(c_{36}+c_{45})}{2}e^{(i)}_{j-k}\right) \\
&\quad \times (k+2)(k+1)\widehat{C}^{(i)}_{k+2} + \left(e_{16}g^{(i)}_{j-k} + e_{34}f^{(i)}_{j-k} + \frac{(e_{36}+e_{14})}{2}e^{(i)}_{j-k}\right) \\
&\quad \times (k+2)(k+1)\widehat{D}^{(i)}_{k+2} + \sum_{k=0}^{j}\Big[(\lambda_m-1)\Big[(c_{44}-c_{66})e^{(i)}_{j-k} - 2c_{46}h^{(i)}_{j-k}\Big] \\
&\quad \times (k+1)\widehat{B}^{(i)}_{k+1} + \Big[\lambda_m((\lambda_m-1)c_{44}+c_{66})g^{(i)}_{j-k} + \lambda_m((\lambda_m-1)c_{66} \\
&\quad + c_{44})f^{(i)}_{j-k} + \lambda_m(2-\lambda_m)c_{46}e^{(i)}_{j-k}\Big]\widehat{B}^{(i)}_k + (\lambda_m-1)\Big[(c_{45}-c_{16})e^{(i)}_{j-k} \\
&\quad - \Big(c_{56}+c_{14})h^{(i)}_{j-k}\Big](k+1)\widehat{A}^{(i)}_{k+1} + \Big[\lambda_m(\lambda_m-1)\times\Big(c_{16}f^{(i)}_{j-k} + c_{45}g^{(i)}_{j-k} \\
&\quad - \frac{(c_{56}+c_{14})}{2}e^{(i)}_{j-k}\Big) + \lambda_m\left(c_{16}g^{(i)}_{j-k} + c_{45}f^{(i)}_{j-k} + \frac{(c_{56}+c_{14})}{2}e^{(i)}_{j-k}\right)\Big]\widehat{A}^{(i)}_k \\
&\quad + \Big(\lambda_m-1)\Big[(c_{34}-c_{56})e^{(i)}_{j-k} - (c_{36}+c_{45})h^{(i)}_{j-k}\Big](k+1)\widehat{C}^{(i)}_{k+1} \\
&\quad + \Big[\lambda_m(\lambda_m-1)\left(c_{56}f^{(i)}_{j-k} + c_{34}g^{(i)}_{j-k} - \frac{(c_{36}+c_{45})}{2}e^{(i)}_{j-k}\right) \\
&\quad + \lambda_m\left(c_{56}g^{(i)}_{j-k} + c_{34}f^{(i)}_{j-k} + \frac{(c_{36}+c_{45})}{2}e^{(i)}_{j-k}\right)\Big]\widehat{C}^{(i)}_k \\
&\quad + (\lambda_m-1)\Big[(e_{34}-e_{16})e^{(i)}_{j-k} - (e_{36}+e_{14})h^{(i)}_{j-k}\Big](k+1)\widehat{D}^{(i)}_{k+1} \\
&\quad + \Big[\lambda_m(\lambda_m-1)\left(e_{16}f^{(i)}_{j-k} + e_{34}g^{(i)}_{j-k} - \frac{(e_{36}+e_{14})}{2}e^{(i)}_{j-k}\right) \\
&\quad + \lambda_m\left(e_{16}g^{(i)}_{j-k} + e_{34}f^{(i)}_{j-k} + \frac{(e_{36}+e_{14})}{2}e^{(i)}_{j-k}\right)\Big]\widehat{D}^{(i)}_k\Big]\Bigg\},
\end{aligned}
\tag{14b}
$$

$$
\begin{aligned}
&\widehat{C}^{(i)}_{j+2} + \left(c_{15}n^{(i)}_0 + c_{35}m^{(i)}_0 + \frac{(c_{13}+c_{55})}{2}l^{(i)}_0\right)\widehat{A}^{(i)}_{j+2} \\
&\quad + \left(c_{56}n^{(i)}_0 + c_{34}m^{(i)}_0 + \frac{(c_{36}+c_{45})}{2}l^{(i)}_0\right)\widehat{B}^{(i)}_{j+2} \\
&\quad + \left(e_{15}n^{(i)}_0 + e_{33}m^{(i)}_0 + \frac{(e_{13}+e_{35})}{2}l^{(i)}_0\right)\widehat{D}^{(i)}_{j+2} \\
&= \frac{-1}{(j+2)(j+1)}\Bigg\{\sum_{k=0}^{j-1}\Bigg[\Bigg(c_{15}n^{(i)}_{j-k} + c_{35}m^{(i)}_{j-k} + \frac{(c_{13}+c_{55})}{2}l^{(i)}_{j-k}\Bigg) \\
&\quad \times (k+2)(k+1)\widehat{A}^{(i)}_{k+2} + \left(c_{56}n^{(i)}_{j-k} + 2 + c_{34}m^{(i)}_{j-k} + \frac{(c_{36}+c_{45})}{2}l^{(i)}_{j-k}\right)\Bigg] \\
&\quad \times (k+2)(k+1)\widehat{B}^{(i)}_{k+2} + \left(e_{15}n^{(i)}_{j-k} + e_{33}m^{(i)}_{j-k} + \frac{(e_{13}+e_{35})}{2}l^{(i)}_{j-k}\right) \\
&\quad \times (k+2)(k+1)\widehat{D}^{(i)}_{k+2} + \sum_{k=0}^{j}\Big[(\lambda_m-1)\Big[(c_{33}-c_{55})l^{(i)}_{j-k} - 2c_{35}o^{(i)}_{j-k}\Big] \\
&\quad \times (k+1)\widehat{C}^{(i)}_{k+1} + \Big[\lambda_m((\lambda_m-1)c_{33}+c_{55})n^{(i)}_{j-k} + \lambda_m((\lambda_m-1)c_{55} \\
&\quad + c_{33})m^{(i)}_{j-k} + \lambda_m(2-\lambda)c_{35}l^{(i)}_{j-k}\Big]\widehat{C}^{(i)}_k + (\lambda_m-1)\Big[(c_{35}-c_{15})l^{(i)}_{j-k} \\
&\quad - \Big(c_{13}+c_{55})o^{(i)}_{j-k}\Big](k+1)\widehat{A}^{(i)}_{k+1} + \Big[\lambda_m(\lambda_m-1)\times\Big(c_{15}m^{(i)}_{j-k} + c_{35}n^{(i)}_{j-k} \\
&\quad - \frac{(c_{13}+c_{55})}{2}l^{(i)}_{j-k}\Big) + \lambda_m\left(c_{15}n^{(i)}_{j-k} + c_{35}m^{(i)}_{j-k} + \frac{(c_{13}+c_{55})}{2}l^{(i)}_{j-k}\right)\Big]\widehat{A}^{(i)}_k \\
&\quad + (\lambda_m-1)\Big[(c_{34}-c_{56})l^{(i)}_{j-k} - (c_{36}+c_{45})o^{(i)}_{j-k}\Big](k+1)\widehat{B}^{(i)}_{k+1} \\
&\quad + \Big[\lambda_m(\lambda_m-1)\left(c_{56}m^{(i)}_{j-k} + c_{34}n^{(i)}_{j-k} - \frac{(c_{36}+c_{45})}{2}l^{(i)}_{j-k}\right) \\
&\quad + \lambda_m\left(c_{56}n^{(i)}_{j-k} + c_{34}m^{(i)}_{j-k} + \frac{(c_{36}+c_{45})}{2}l^{(i)}_{j-k}\right)\Big]\widehat{B}^{(i)}_k \\
&\quad + \Big(\lambda_m-1)\Big[(e_{33}-e_{15})l^{(i)}_{j-k} - (e_{13}+e_{35})o^{(i)}_{j-k}\Big](k+1)\widehat{D}^{(i)}_{k+1} \\
&\quad + \Big[\lambda_m(\lambda_m-1)\left(e_{15}m^{(i)}_{j-k} + e_{33}n^{(i)}_{j-k} - \frac{(e_{13}+e_{35})}{2}l^{(i)}_{j-k}\right) \\
&\quad + \lambda_m\left(e_{15}n^{(i)}_{j-k} + e_{33}m^{(i)}_{j-k} + \frac{(e_{13}+e_{35})}{2}l^{(i)}_{j-k}\right)\Big]\widehat{D}^{(i)}_k\Big]\Bigg\},
\end{aligned}
\tag{14c}
$$

$$
\begin{aligned}
&\widehat{D}^{(i)}_{j+2} - \left(e_{11}r^{(i)}_0 + e_{35}q^{(i)}_0 + \frac{(e_{15}+e_{31})}{2}p^{(i)}_0\right)\widehat{A}^{(i)}_{j+2} \\
&\quad - \left(e_{16}r^{(i)}_0 + e_{34}q^{(i)}_0 + \frac{(e_{14}+e_{36})}{2}p^{(i)}_0\right)\widehat{B}^{(i)}_{j+2} \\
&\quad - \left(e_{15}r^{(i)}_0 + e_{33}q^{(i)}_0 + \frac{(e_{13}+e_{35})}{2}p^{(i)}_0\right)\widehat{C}^{(i)}_{j+2} \\
&= \frac{-1}{(j+2)(j+1)}\Bigg\{\sum_{k=0}^{j-1}\Bigg[-\Bigg(e_{11}r^{(i)}_{j-k} + e_{35}q^{(i)}_{j-k} + \frac{(e_{15}+e_{31})}{2}p^{(i)}_{j-k}\Bigg) \\
&\quad \times (k+2)(k+1)\widehat{A}^{(i)}_{k+2} - \left(e_{16}r^{(i)}_{j-k} + e_{34}q^{(i)}_{j-k} + \frac{(e_{14}+e_{36})}{2}p^{(i)}_{j-k}\right)\Bigg] \\
&\quad \times (k+2)(k+1)\widehat{B}^{(i)}_{k+2} - \left(e_{15}r^{(i)}_{j-k} + e_{33}q^{(i)}_{j-k} + \frac{(e_{13}+e_{35})}{2}p^{(i)}_{j-k}\right)
\end{aligned}
$$

$$\times (k+2)(k+1)\widehat{C}^{(i)}_{k+2} + \sum_{k=0}^{j}\Big[(\lambda_m-1)\Big[(\eta_{33}-\eta_{11})p^{(i)}_{j-k} - 2\eta_{13}s^{(i)}_{j-k}\Big]$$
$$\times (k+1)\widehat{D}^{(i)}_{k+1} + \Big[\lambda_m((\lambda_m-1)\eta_{33}+\eta_{11})r^{(i)}_{j-k} + \lambda_m((\lambda_m-1)\eta_{11}$$
$$+\eta_{33})q^{(i)}_{j-k} + \lambda_m(2-\lambda_m)\eta_{13}p^{(i)}_{j-k}\Big]\widehat{D}^{(i)}_{k} - (\lambda_m-1)\Big[(e_{35}-e_{11})p^{(i)}_{j-k}$$
$$-(e_{15}+e_{31})s^{(i)}_{j-k}\Big](k+1)\widehat{A}^{(i)}_{k+1} - \Big[\lambda_m(\lambda_m-1)\times\Big(e_{11}q^{(i)}_{j-k} + e_{35}r^{(i)}_{j-k}$$
$$-\frac{(e_{15}+e_{31})}{2}p^{(i)}_{j-k}\Big) + \lambda_m(e_{11}r^{(i)}_{j-k} + e_{35}q^{(i)}_{j-k} + \frac{(e_{15}+e_{31})}{2}p^{(i)}_{j-k})\Big]\widehat{A}^{(i)}_{k}$$
$$-(\lambda_m-1)\Big[(e_{34}-e_{16})p^{(i)}_{j-k} - (e_{14}+e_{36})s^{(i)}_{j-k}\Big](k+1)\widehat{B}^{(i)}_{k+1}$$
$$-\Big[\lambda_m(\lambda_m-1)\Big(e_{16}q^{(i)}_{j-k} + e_{34}r^{(i)}_{j-k} - \frac{(e_{14}+e_{36})}{2}p^{(i)}_{j-k}\Big)$$
$$+\lambda_m(e_{16}r^{(i)}_{j-k} + e_{34}q^{(i)}_{j-k} + \frac{(e_{14}+e_{36})}{2}p^{(i)}_{j-k})\Big]\widehat{B}^{(i)}_{k}$$
$$-(\lambda_m-1)\Big[(e_{33}-e_{15})p^{(i)}_{j-k} - (e_{13}+e_{35})s^{(i)}_{j-k}\Big](k+1)\widehat{C}^{(i)}_{k+1}$$
$$-\Big[\lambda_m(\lambda_m-1)\Big(e_{15}q^{(i)}_{j-k} + e_{33}r^{(i)}_{j-k} - \frac{(e_{13}+e_{35})}{2}p^{(i)}_{j-k}\Big)$$
$$+\lambda_m\Big(e_{15}r^{(i)}_{j-k} + e_{33}q^{(i)}_{j-k} + \frac{(e_{13}+e_{35})}{2}p^{(i)}_{j-k}\Big)\Big]\widehat{C}^{(i)}_{k}\Big]\Big\}. \tag{14d}$$

If $\widehat{A}^{(i)}_0, \widehat{A}^{(i)}_1, \widehat{B}^{(i)}_0, \widehat{B}^{(i)}_1, \widehat{C}^{(i)}_0, \widehat{C}^{(i)}_1, \widehat{D}^{(i)}_0$ and $\widehat{D}^{(i)}_1$ are known, then $\widehat{A}^{(i)}_{j+2}, \widehat{B}^{(i)}_{j+2}, \widehat{C}^{(i)}_{j+2}$ and $\widehat{D}^{(i)}_{j+2}$ can be determined using Eqs. (14). Hence, the solutions of Eqs. (11) in subdomain i can be simply represented as,

$$\widehat{U}^{(m)}_{0i}(\theta,\varphi) = \widehat{A}^{(i)}_0\widehat{U}^{(m)}_{0i0} + \widehat{A}^{(i)}_1\widehat{U}^{(m)}_{0i1} + \widehat{B}^{(i)}_0\widehat{U}^{(m)}_{0i2} + \widehat{B}^{(i)}_1\widehat{U}^{(m)}_{0i3} + \widehat{C}^{(i)}_0\widehat{U}^{(m)}_{0i4} + \widehat{C}^{(i)}_1\widehat{U}^{(m)}_{0i5} + \widehat{D}^{(i)}_0\widehat{U}^{(m)}_{0i6} + \widehat{D}^{(i)}_1\widehat{U}^{(m)}_{0i7},$$
$$\widehat{V}^{(m)}_{0i}(\theta,\varphi) = \widehat{A}^{(i)}_0\widehat{V}^{(m)}_{0i0} + \widehat{A}^{(i)}_1\widehat{V}^{(m)}_{0i1} + \widehat{B}^{(i)}_0\widehat{V}^{(m)}_{0i2} + \widehat{B}^{(i)}_1\widehat{V}^{(m)}_{0i3} + \widehat{C}^{(i)}_0\widehat{V}^{(m)}_{0i4} + \widehat{C}^{(i)}_1\widehat{V}^{(m)}_{0i5} + \widehat{D}^{(i)}_0\widehat{V}^{(m)}_{0i6} + \widehat{D}^{(i)}_1\widehat{V}^{(m)}_{0i7},$$
$$\widehat{W}^{(m)}_{0i}(\theta,\varphi) = \widehat{A}^{(i)}_0\widehat{W}^{(m)}_{0i0} + \widehat{A}^{(i)}_1\widehat{W}^{(m)}_{0i1} + \widehat{B}^{(i)}_0\widehat{W}^{(m)}_{0i2} + \widehat{B}^{(i)}_1\widehat{W}^{(m)}_{0i3} + \widehat{C}^{(i)}_0\widehat{W}^{(m)}_{0i4} + \widehat{C}^{(i)}_1\widehat{W}^{(m)}_{0i5} + \widehat{D}^{(i)}_1\widehat{W}^{(m)}_{0i6} + \widehat{D}^{(i)}_1\widehat{W}^{(m)}_{0i7},$$
$$\widehat{\Phi}^{(m)}_{0i}(\theta,\varphi) = \widehat{A}^{(i)}_0\widehat{\Phi}^{(m)}_{0i0} + \widehat{A}^{(i)}_1\widehat{\Phi}^{(m)}_{0i1} + \widehat{B}^{(i)}_0\widehat{\Phi}^{(m)}_{0i2} + \widehat{B}^{(i)}_1\widehat{\Phi}^{(m)}_{0i3} + \widehat{C}^{(i)}_0\widehat{\Phi}^{(m)}_{0i4} + \widehat{C}^{(i)}_1\widehat{\Phi}^{(m)}_{0i5} + \widehat{D}^{(i)}_0\widehat{\Phi}^{(m)}_{0i6} + \widehat{D}^{(i)}_1\widehat{\Phi}^{(m)}_{0i7}. \tag{15}$$

To obtain the solutions of Eqs. (11) for the whole domain of φ, the following continuity conditions at the interface ($\varphi = \varphi_i$) between sub-domains $i$and $i+1$ have to be satisfied;

$$\sigma^{(i)}_{rr}(\rho,\theta,\varphi_i)\sin\varphi_i + \sigma^{(i)}_{rz}(\rho,\theta,\varphi_i)\cos\varphi_i = \sigma^{(i+1)}_{rr}(\rho,\theta,\varphi_i)\sin\varphi_i + \sigma^{(i+1)}_{rz}(\rho,\theta,\varphi_i)\cos\varphi_i, \tag{16a}$$
$$\sigma^{(i)}_{rz}(\rho,\theta,\varphi_i)\sin\varphi_i + \sigma^{(i)}_{zz}(\rho,\theta,\varphi_i)\cos\varphi_i = \sigma^{(i+1)}_{rz}(\rho,\theta,\varphi_i)\sin\varphi_i + \sigma^{(i+1)}_{zz}(\rho,\theta,\varphi_i)\cos\varphi_i, \tag{16b}$$
$$\sigma^{(i)}_{\theta r}(\rho,\theta,\varphi_i)\sin\varphi_i + \sigma^{(i)}_{\theta z}(\rho,\theta,\varphi_i)\cos\varphi_i = \sigma^{(i+1)}_{\theta r}(\rho,\theta,\varphi_i)\sin\varphi_i + \sigma^{(i+1)}_{\theta z}(\rho,\theta,\varphi_i)\cos\varphi_i, \tag{16c}$$
$$D^{(i)}_{r}(\rho,\theta,\varphi_i)\sin\varphi_i + D^{(i)}_{z}(\rho,\theta,\varphi_i)\cos\varphi_i = D^{(i+1)}_{r}(\rho,\theta,\varphi_i)\sin\varphi_i + D^{(i+1)}_{z}(\rho,\theta,\varphi_i)\cos\varphi_i, \tag{16d}$$
$$u^{(i)}_r(\rho,\theta,\varphi_i) = u^{(i+1)}_r(\rho,\theta,\varphi_i), \tag{16e}$$
$$u^{(i)}_\theta(\rho,\theta,\varphi_i) = u^{(i+1)}_\theta(\rho,\theta,\varphi_i), \tag{16f}$$
$$u^{(i)}_z(\rho,\theta,\varphi_i) = u^{(i+1)}_z(\rho,\theta,\varphi_i), \tag{16g}$$
$$\phi^{(i)}(\rho,\theta,\varphi_i) = \phi^{(i+1)}(\rho,\theta,\varphi_i). \tag{16h}$$

If the domain of φ under consideration is divided into n sub-domains (Fig. 3), the $8n$ coefficients in Eq. (15) for $i = 1,2,\ldots,n$, must be determined. The interface continuity conditions yield $8(n-1)$ equations (Eqs. (16) with $i = 1,2,\ldots,(n-1)$). The homogenous boundary conditions at $\varphi = \varphi_0$ and $\varphi = \varphi_n$ yield another eight equations. In total, $8n$ homogeneous algebraic equations for these $8n$ coefficients can thus be constructed. A nontrivial solution yields an $8n \times 8n$ determinant of zero. The roots of the zero determinant (λ_m) can be complex numbers, and were obtained herein using the subroutine, "DZANLY", in IMSL (International Mathematical and Statistical Library). The subroutine is based on the numerical approach of Müller [31].

Two types of mechanical boundary condition were considered herein – free and clamped. For free traction at $\varphi = \varphi_0$ or $\varphi = \varphi_n$,

$$\sigma_{rr}\sin\varphi + \sigma_{rz}\cos\varphi = 0, \quad \sigma_{rz}\sin\varphi + \sigma_{zz}\cos\varphi = 0,$$
$$\sigma_{\theta r}\sin\varphi + \sigma_{\theta z}\cos\varphi = 0$$

while the clamped boundary conditions require $u_r = u_z = u_\theta = 0$. Two types of electric boundary conditions can also be specified at $\varphi = \varphi_0$ or $\varphi = \varphi_n$. They are electrically open and closed boundary conditions. Electrically open and closed conditions are $D_r\sin\varphi + D_z\cos\varphi = 0$ and $\phi = 0$, respectively.

4. Convergence and Comparison

The convergence and comparison of the minimum Re[λ_m] (real part of λ_m) of bi-material bodies of revolution are summarized here to confirm the correctness of the proposed solutions. Two geometric shapes with a horizontal interface, called geometry I and geometry II, displayed in Fig. 4, are considered. Geometry I has $\varphi_0 = 90°$ and $\varphi_n = 270°$ while geometry II has $\varphi_0 = 0°$ and $\varphi_n = 270°$, as shown in Fig. 3. Table 1 gives the material constants, and the direction of polarization of the material is assumed to be along the axis of revolution ($\gamma = 0°$). Notably, material PZT-6B (Im.) in Table 1 is an imaginary material with the same elastic properties as PZT-6B, and is adopted here to obtain results that can be compared with those of Xu and Mutoh [27]. The boundary conditions at $\varphi = \varphi_0$ and $\varphi = \varphi_n$ are traction-free and electrically open.

Table 2 lists the minimum values of Re[λ_m] that were obtained by dividing the domain of φ into various numbers of sub-domains of equal size, using different numbers of terms in the series solution for each sub-domain. Notably, the λ_m, which correspond to minimum of Re[λ_m], are all real in the cases considered in Table 2. The convergent solutions can be obtained by fixing the number of sub-domains and increasing the number of terms in series solutions or by fixing the number of terms in series solutions and increasing the number of sub-domains. The results published in Xu and Mutoh [27] and Li et al. [29], which were obtained based on the assumption of axisymmetric deformation, are also given in Table 2. The excellent agreement between the convergent results herein and the published data validates the proposed solutions.

5. Numerical results and discussion

The electroelastic singularity is governed by the real part of (λ_m-1), and the root of primary interest is the one with the smallest positive real part between zero and one. In this section, the values of minimum Re[λ_m] are shown for single material and bi-material bodies of revolution. The piezoelectric materials, PZT-4 and PZT-5H, and an elastic material, Al (aluminium), are considered. The material properties of PZT-4 and PZT-5H are given in Table 1, while the elastic constants for Al are E (Young's modulus) = 68.9 GPa and ν (Poisson's ratio) = 0.25. The results were obtained using eight equal sub-domains for φ and 15-term series solutions for each sub-domain. The boundary conditions under consideration are specified by four letters. The first pair of letters refers to the boundary conditions at $\varphi = \varphi_0$, while the second pair specifies the boundary conditions at $\varphi = \varphi_n$. The first letter in each pair concerns the mechanical boundary conditions, with C and F's denoting clamped and free boundary conditions, respectively, while the second letter concerns the electric boundary conditions with C and O's representing electrically closed and open boundary conditions, respectively. Accordingly, in the following, COFO boundary conditions mean that the mechanical boundary conditions are clamped and free at $\varphi = \varphi_0$ and $\varphi = \varphi_n$, respectively, and the electric boundary conditions are open at $\varphi = \varphi_0$ and $\varphi = \varphi_n$.

5.1. Bodies of revolution made of a single piezoelectric material

Consider a PZT-4 or PZT-5H body of revolution with a direction of polarization that my not be along the Z-axis (axis of revolution). The geometry of the body considered in this section is similar to geometry II in Fig. 4. Figs. 5 plots the variations of minimum Re[λ_m] with θ for PZT-4 bodies with $\gamma = 0°$, 45° and 90°, while Fig. 6 plots corresponding curves for PZT-5H bodies. Notably, the results at $\theta = 2\pi - \theta_0$ are identical to those at $\theta = \theta_0$ in all the cases that are considered in this work. Consequently, the range of θ considered is between 0° and 180°. The λ_m that corresponds to minimum Re[λ_m] are all real in the cases examined in Figs. 5 and 6.

As expected, minimum Re[λ_m] does not change with θ when the direction of polarization is along the Z-axis ($\gamma = 0°$). When the direction of polarization is not along the Z-axis, minimum Re[λ_m] varies significantly with θ. For example, when $\gamma = 45°$, the maximum relative difference may reach 7.8% for a PZT-4 body with COCO boundary conditions, while the maximum difference is

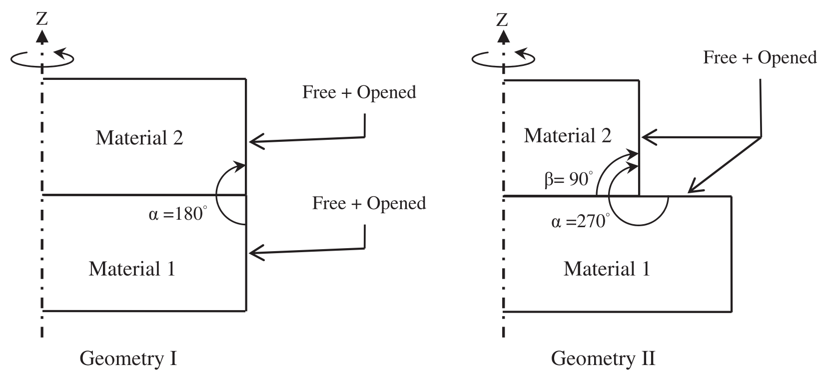

Fig. 4. Geometry and boundary conditions for bodies of revolution considered in convergence studies.

Table 1
Material properties of piezoelectric materials.

Material	Stiffness [GPa]					Piezoelectric const. [C/m^2]			Dielectric const. $\times 10^{-10}$[F/m]	
	$\bar{c}_{11}$	$\bar{c}_{12}$	$\bar{c}_{13}$	$\bar{c}_{33}$	$\bar{c}_{44}$	$\bar{e}_{15}$	$\bar{e}_{31}$	$\bar{e}_{33}$	$\bar{\eta}_{11}$	$\bar{\eta}_{33}$
CdSe	74.1	45.2	39.3	83.6	13.2	−0.138	−0.159	0.347	0.844	0.903
PZT-4	139.0	77.8	74.3	115.0	25.6	12.7	−5.2	15.1	64.6	56.2
PZT-5H	126.0	55.0	53.0	117.0	35.3	17.0	−6.5	23.3	151.0	130.0
PZT-6B	168.0	60.0	60.0	163.0	27.1	4.6	−0.9	7.1	36.0	34.0
$BaTiO_3$	275.0	179.0	152.0	165.0	54.3	21.3	−2.69	3.65	175.0	9.88
PZT-6B (Im.)	168.0	60.0	60.0	163.0	27.1	43.0	−14.0	36.0	200.0	247.0

Table 2
Convergence of minimum Re[λ_m].

Geometry	Material 1/Material 2	Number of Sub-domains	Number of Polynomial terms							Published results [27]*, [29]⁺
			5	6	7	9	11	13	15	
I	CdSe/ PZT-5H	2	0.9363	0.9348	0.9357	0.9377	0.9387	0.9383	0.9380	0.9381*
		4	0.9379	0.9381	0.9382	0.9381	0.9381	0.9381	0.9381	
		6	0.9381	0.9381	0.9381	0.9381	0.9381	0.9381	0.9381	
		8	0.9381	0.9381	0.9381	0.9381	0.9381	0.9381	0.9381	
	CdSe/ PZT-6B	2	0.9268	0.9242	0.9308	0.9302	0.9280	0.9272	0.9278	0.9281*
		4	0.9286	0.9289	0.9279	0.9281	0.9281	0.9281	0.9281	
		6	0.9281	0.9281	0.9281	0.9281	0.9281	0.9281	0.9281	
		8	0.9281	0.9281	0.9281	0.9281	0.9281	0.9281	0.9281	
	CdSe/ $BaTiO_3$	2	0.8949	0.9588	0.9429	0.9172	0.9394	0.9256	0.9284	0.9429*
		4	0.9436	0.9430	0.9430	0.9430	0.9429	0.9429	0.9429	
		6	0.9429	0.9428	0.9428	0.9429	0.9429	0.9429	0.9429	
		8	0.9429	0.9428	0.9429	0.9429	0.9429	0.9429	0.9429	
	PZT-6B/ PZT-6B (Im.)	2	0.98792	0.98475	0.98641	0.98793	0.98713	0.98828	0.98792	0.98724⁺
		4	0.98742	0.98732	0.98731	0.98720	0.98613	0.98725	0.98724	
		6	0.98802	0.98764	0.98764	0.98733	0.98724	0.98724	0.98724	
		8	0.98730	0.98724	0.98723	0.98724	0.98724	0.98724	0.98724	
II	PZT-6B/ PZT-6B (Im.)	3	0.54766	0.53669	0.52792	0.52053	0.52716	0.52670	0.53197	0.52819⁺
		6	0.52694	0.52758	0.52801	0.52836	0.52819	0.52818	0.52820	
		9	0.52803	0.52809	0.52823	0.52820	0.52820	0.52820	0.52820	

⁺ means that the results are from reference [29].
* means that the results are from reference [27].

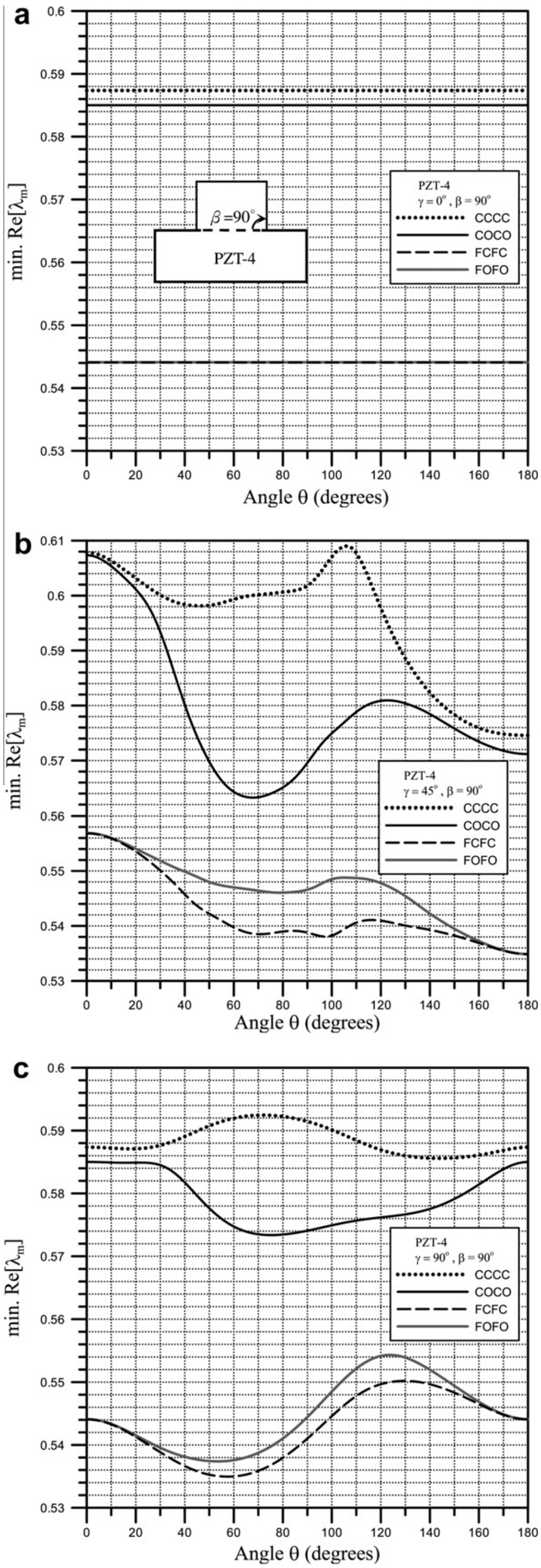

Fig. 5. Variation of minimun Re[λ_m] with θ for PZT-4 of bodis of revolution with $\beta = 90°$: (a) $\gamma = 0°$, (b) $\gamma = 45°$, (c) $\gamma = 90°$.

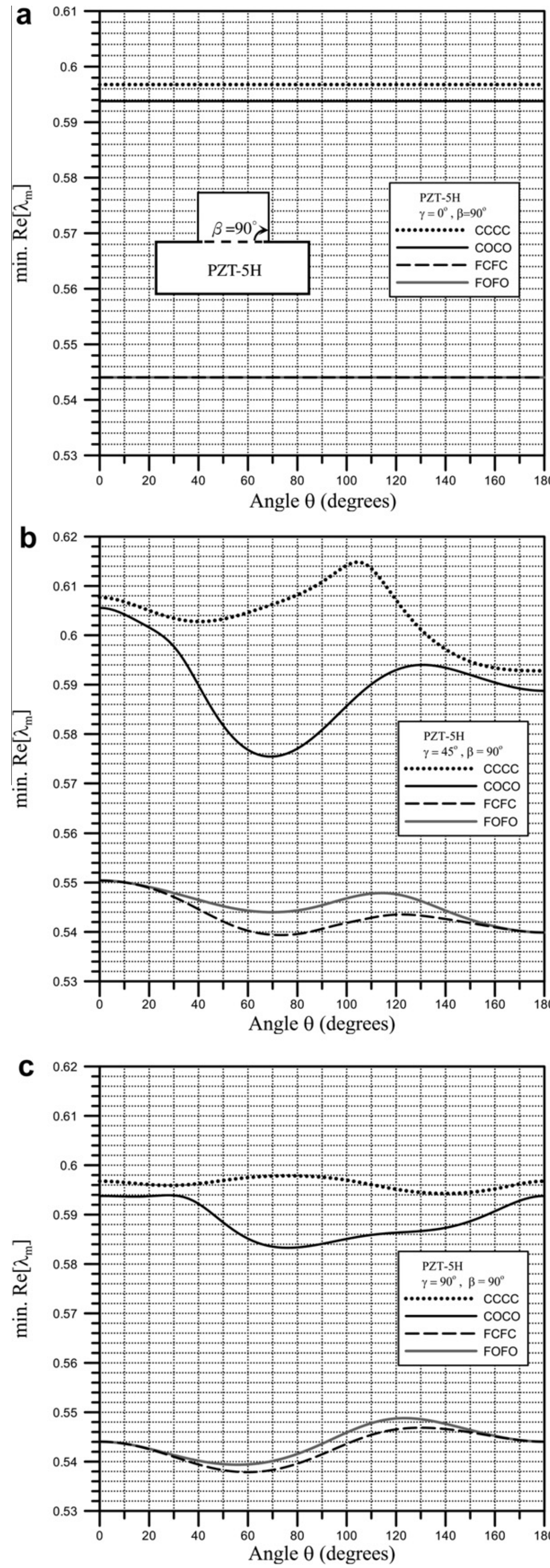

Fig. 6. Variation of minimun Re[λ_m] with θ for PZT-5H of bodis of revolution with $\beta = 90°$: (a) $\gamma = 0°$, (b) $\gamma = 45°$, (c) $\gamma = 90°$.

about 5.2 % for a PZT-5H body. When γ changes from 0° to 45° or 90°, the minimum Re[λ_m] may increase or decrease, depending on the values of θ and the boundary conditions. PZT-4 bodies exhibit more severe electroelastic singularities than PZT-5H bodies under clamped–clamped mechanical boundary conditions; the opposite is true under free-free mechanical boundary conditions.

Figs. 7 and 8 display the variations in minimum Re[λ_m] at θ = 60° with β for PZT-4 and PZT-5H bodies, respectively. Two values of γ, 0°and 45°, were considered. Generally, minimum Re[λ_m] declines as β increases, such that a larger β induces more severe electroelastic singularities at the sharp corner of a body of revolution. Electroelastic singularities under free-free boundary conditions are more severe than those obtained under clamped–clamped boundary conditions. When γ = 0°, the electric boundary conditions do not significantly affect the singularities. However, when γ = 45°, open-open electric boundary conditions results in a smaller minimum Re[λ_m] than closed-closed electric boundary conditions for clamped–clamped bodies of revolution, while the opposite trend is true for bodies of revolution with free-free mechanical boundary conditions. As γ changes from 0° to 45°, the λ_m, which corresponds to minimum Re[λ_m], may change from real to complex or from complex to real. For instance, under CCCC boundary conditions, λ_m are complex for γ = 45° when β is between 48° and 73° for PZT-4 bodies and between 52° and 70° for PZT-5H bodies, while they are all real for γ = 0°. A comparison of Figs. 7 and 8 reveals that PZT-4 bodies have stronger singularities than PZT-5H bodies under clamped–clamped boundary conditions, but not at all values of β under free-free boundary conditions.

5.2. Bi-material bodies of revolution made of piezoelectric and elastic materials

This section investigates bi-material bodies of revolution with a geometry that is similar to geometry II in Fig. 4, in which material 1 is an isotropic elastic material, Al, and material 2 is PZT-4 or PZT-5H. The arrangements considered in Figs. 9–12 are the same as those in Figs. 5–7, respectively, except that bi-material bodies of revolution are considered in Figs. 9–12. Notably, the continuity conditions on the interface between the piezoelectric material and the elastic material are given by Eqs. (16) and $\phi^{(i+1)}(\rho,\theta,\varphi_i) = 0$. No electric boundary condition applies at $\varphi = \varphi_0$, and the second letter of the four letters that denote the boundary conditions is replaced by "–".

Figs. 9 and 10 discover that when $\gamma \neq 0°$, the minimum Re[λ_m] does significantly vary with θ. When γ = 45°, the maximum relative

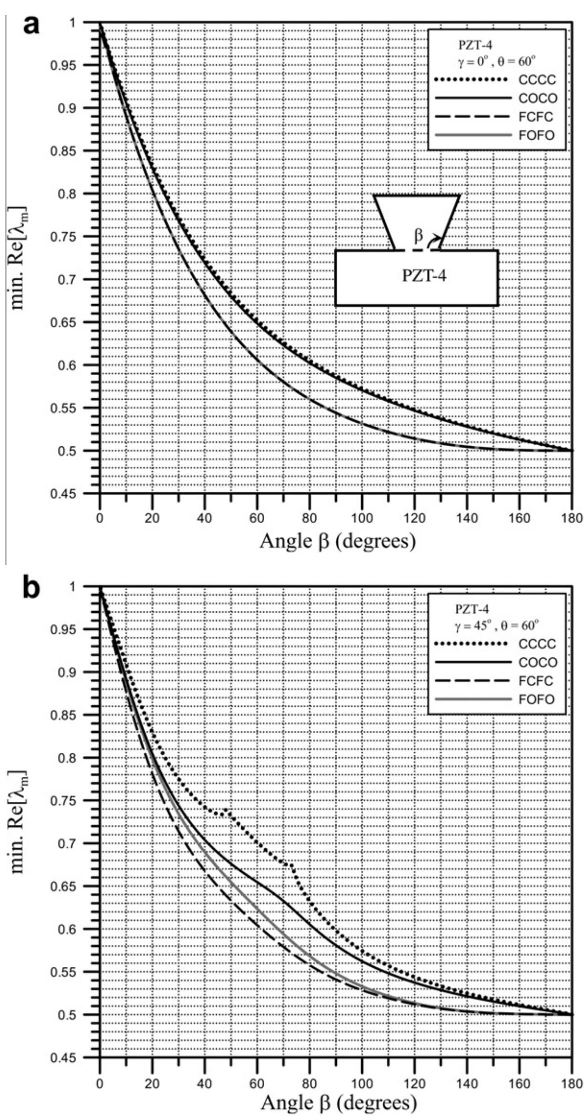

Fig. 7. Variation of minimum Re[λ_m] at θ = 60° with β for PZT-4 bodies of revolution: (a) γ = 0°, (b) γ = 45°.

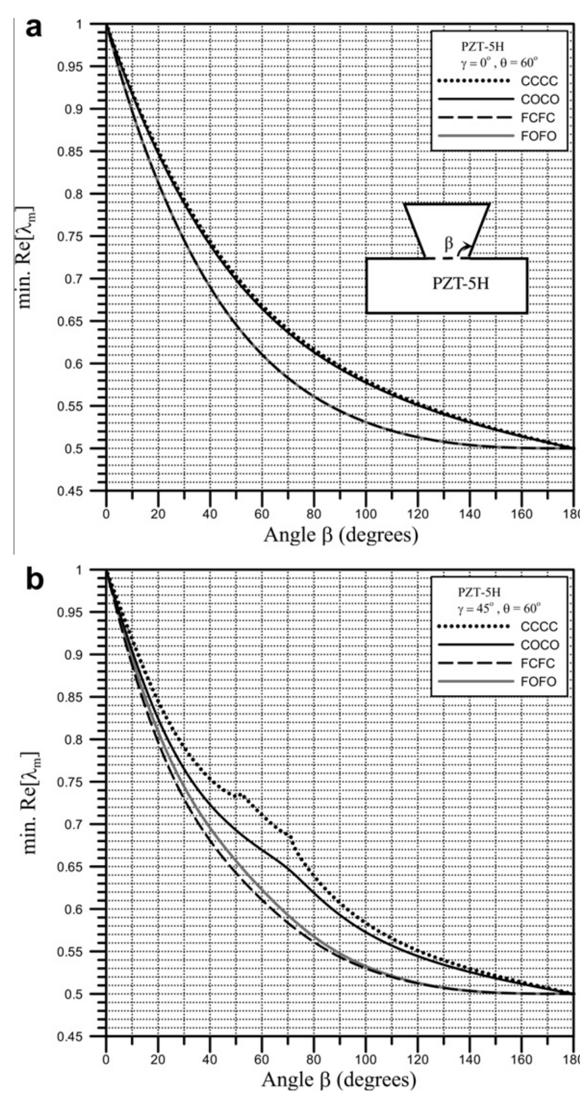

Fig. 8. Variation of minimum Re[λ_m] at θ = 60° with β for PZT-5H bodies of revolution: (a) γ = 0°, (b) γ = 45°.

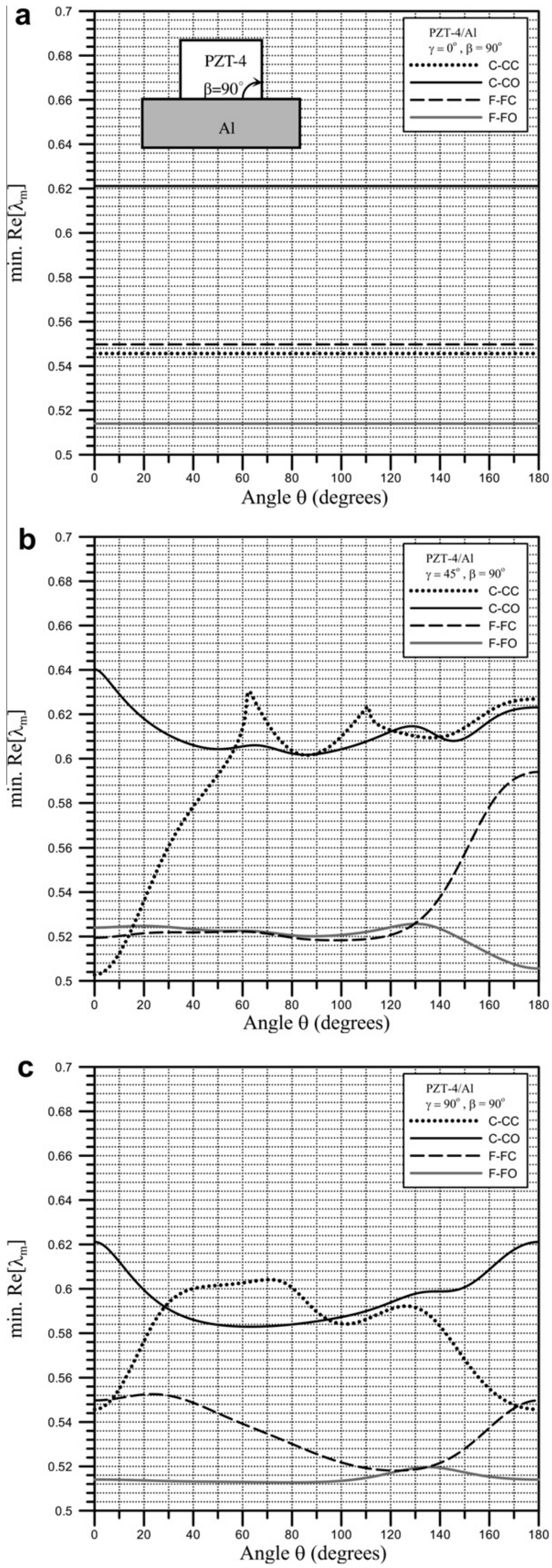

Fig. 9. Variation of minimun Re[λ_m] with θ for PZT-4/Al of bodis of revolution with β = 90°: (a) γ = 0°, (b) γ = 45°, (c) γ = 90°.

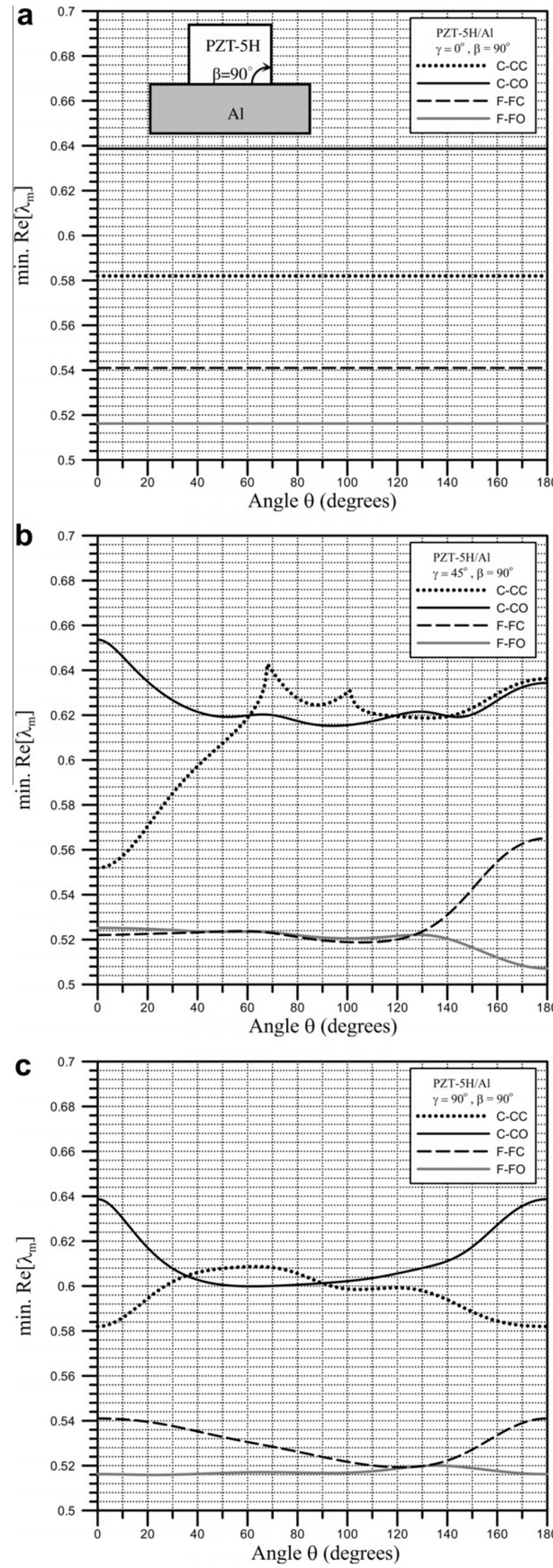

Fig. 10. Variation of minimun Re[λ_m] with θ for PZT-5H/Al of bodis of revolution with β = 90°: (a) γ = 0°, (b) γ = 45°, (c) γ = 90°.

difference may reach 25% for a PZT-4/Al body under C-CC boundary conditions, while the maximum difference is approximately 16 % for a PZT-5H/Al body. Unlike in Figs. 5 and 6, the minimum Re[λ_m] for the C-CC boundary conditions can be smaller than those for C-

CO boundary conditions, depending on γ and θ. When $\gamma = 45°$, the λ_m, which correspond to minimum Re[λ_m] under C-CC boundary conditions, are no longer all real; they are complex for $63° \leqslant \theta \leqslant 110°$ in Fig. 9(b) and $68° \leqslant \theta \leqslant 101°$ in Fig. 10(b). Fig. 9(b) demonstrates that the minimum Re[λ_m] under C-CC boundary conditions are lower than those under free-free boundary conditions when $\theta \leqslant 14°$.

Figs. 11 and 12 plot the variations of minimum Re[λ_m] at $\theta = 60°$with β for PZT-4/Al and PZT-5H/Al bodies, respectively. The relatively abrupt changes in the curves (i.e., at$\beta \approx 159°$ under F-FC boundary conditions and $\beta \approx 99°$ under C-CO boundary conditions in Fig. 11(a)) are caused by the roots's changing from real to complex numbers or from complex to real numbers. Generally, the strength of the electroelastic singularity increases with β. Free-free boundary conditions produce singularities that are more severe than clamped–clamped boundary conditions do, except for-$\beta \geqslant 160°$. Interestingly, the minimum Re[λ_m] for the bodies with $\gamma = 0°$are more considerably affected by electric boundary conditions than those for the bodies with $\gamma = 45°$. Changing γ from 0° to 45° can alter the minimum Re[λ_m] with the maximum relative difference of 9.6% occurring at $\beta = 99°$ under C-CO boundary conditions in Fig. 11. Unlike the minimum Re[λ_m] $\geqslant 0.5$ for bodies of revolution made of two isotropic elastic materials under free-free boundary conditions given in Huang and Leissa [26], the minimum Re[λ_m] can be smaller than 0.5 for β larger than around 150°under F-FO boundary conditions.

5.3. Bi-material bodies of revolution made of piezoelectric materials

The results for bi-material bodies of revolution consisting of PZT-4 and PZT-5H with a horizontal interface are given in Figs. 13 and 14. Fig. 13 concerns bodies of revolution with geometry I and geometry II displayed in Fig. 4, where materials 1 and 2 are PZT-5H and PZT-4, respectively. Fig. 14 considers bodies of revolution with geometry II and having various β.

As expected, Fig. 13 demonstrates that bodies of revolution with geometry II ($\alpha = 270°$) have more severe singularities at the interface corner than do bodies of revolution with geometry I ($\alpha = 180°$). When $\gamma = 0°$, the roots corresponding to minimum Re[λ_m] are all real. As γ changes from 0° to 45° or 90°, the roots may change from real to complex, depending on θ and the boundary conditions. For instance, for $\gamma = 45°$and under COCO boundary conditions, when $\theta < 51°$ and $\theta < 36°$ for geometries I and II, respectively, the roots corresponding to minimum Re[λ_m] are complex.

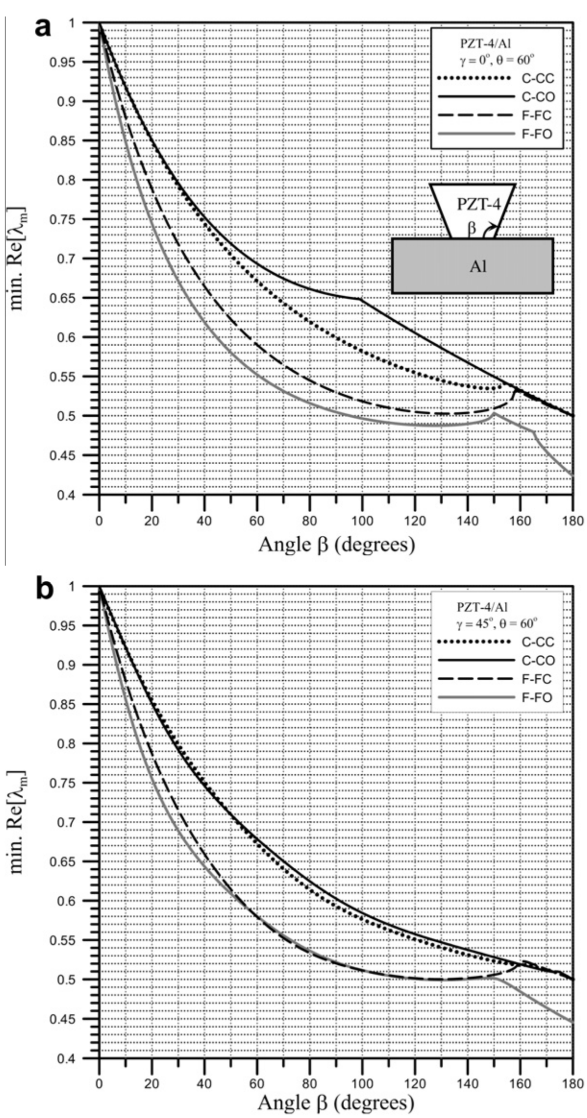

Fig. 11. Variation of minimun Re[λ_m] at $\theta = 60°$ with β for PZT-4/Al bodies of revolution: (a) $\gamma = 0°$, (b) $\gamma = 45°$.

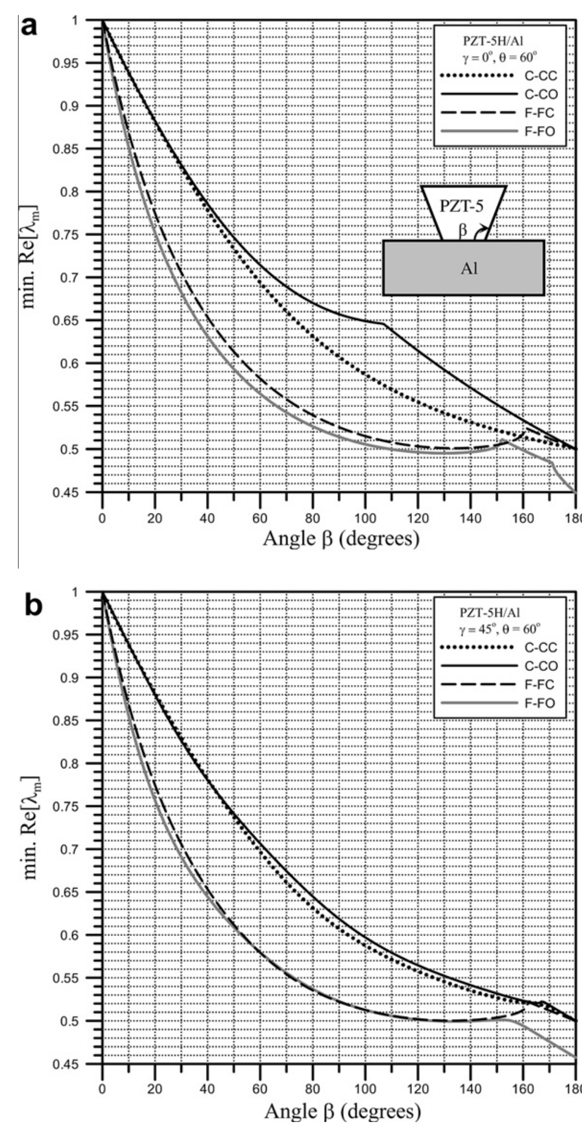

Fig. 12. Variation of minimun Re[λ_m] at $\theta = 60°$ with β for PZT-5H/Al bodies of revolution: (a) $\gamma = 0°$, (b) $\gamma = 45°$.

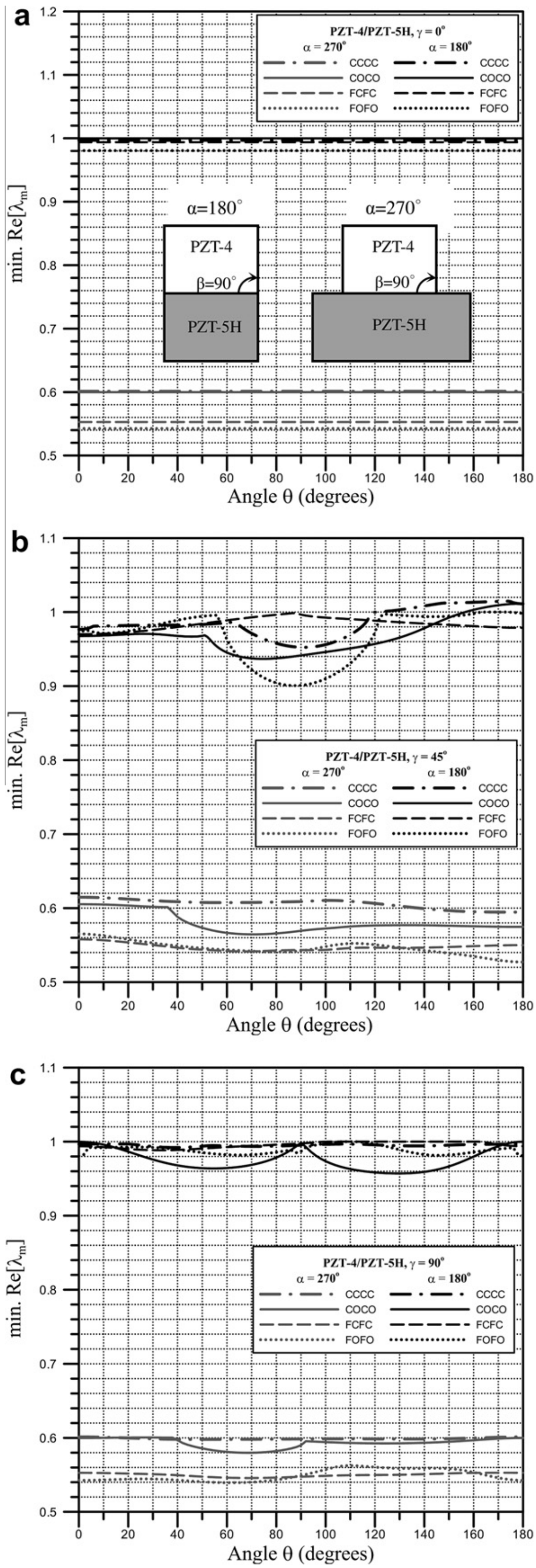

Fig. 13. Variation of minimun Re[λ_m] with θ for PZT-4/ PZT-5H of bodis of revolution with β = 90°: (a) γ = 0°, (b) γ = 45°, (c) γ = 90°.

The variations of minimum Re[λ_m] with θ in Fig. 13(b) indicate that the maximum difference can reach 11% for geometry I under FOFO boundary conditions, and 7.2% for geometry II under FOFO boundary conditions. When γ = 90°, the maximum difference between values of minimum Re[λ_m] for various θ reaches 4.5% for geometry I under COCO boundary conditions, and 4.3% for geometry II under FOFO boundary conditions.

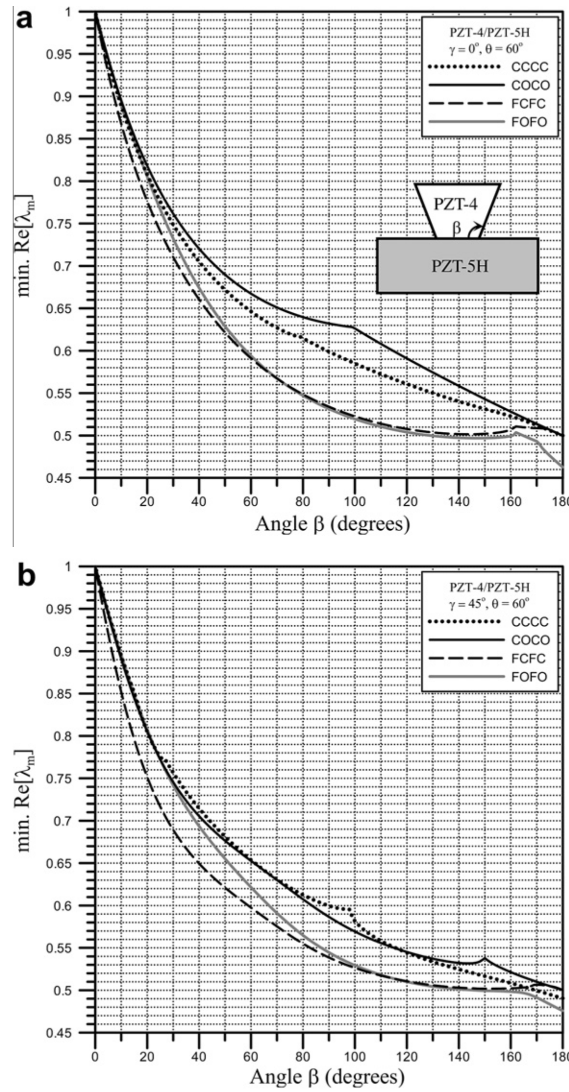

Fig. 14. Variation of minimun Re[λ_m] at θ = 60° with β for PZT-4/ PZT-5H bodies of revolution: (a) γ0°, (b) γ = 45°.

Fig. 14 plots the variations of minimum Re[λ_m] at θ = 60° with β for bodies of revolution with geometry II. Two values of γ, 0°and 45°, were considered. Again, the relatively abrupt changes in the curves are caused by a change in the roots from real to complex or from complex to real. Generally, free-free boundary conditions give more severe singularities at the interface corner than do clamped–clamped boundary conditions. Changing γ from 0° to 45° changes the minimum Re[λ_m] by up to 5.0%, as for the body of revolution with β = 105° under COCO boundary conditions.

6. Concluding remarks

This study developed a general solution for determining electroelastic singularities in piezoelectric bodies of revolution with a direction of polarization that may not be parallel to the axis of revolution. The piezoelectric material is assumed to be transversely isotropic. The eigenfunction expansion approach was combined with a power series solution technique to solve the three-dimensional equilibrium and Maxwell's equations that are presented in terms of displacement components and electric potential. The solution incorporates no auxiliary functions such as stress functions or displacement potential. The present solution is very easily extended to isotropic elastic materials by discarding the piezoelectric constants and dielectric constants and properly setting the elastic constants. The correctness of the proposed solution is verified by comparing the results herein with the published results for cases in which the direction of polarization is along the axis of revolution.

When the direction of polarization of the piezoelectric material is not along the axis of revolution, the assumption of axisymmetric deformation, which was made in published studies of electroelastic singularities in bodies of revolution, is invalid. The numerical results in this work for bodies of revolution, which comprise single piezoelectric material, bonded piezo/piezo or piezo/isotropic elastic materials, reveal that the geometrically induced electroelastic singularity order can depend significantly on the polarized direction and the circular coordinate variable (θ). This is the first study to present numerical results for cases in which the direction of polarization is not parallel to the axis of revolution.

Acknowledgement

This work reported herein was supported by the National Science Council, Taiwan through research Grant No. NSC98-2221-E-009-075-MY3. This support is gratefully acknowledged.

Appendix A

$$[c] = [\mathbf{T}]_\sigma[\mathbf{K}][\bar{c}][\mathbf{K}]^T[\mathbf{T}]_\varepsilon^{-1}, \quad [e] = [\mathbf{T}]_D[\mathbf{L}][\bar{e}][\mathbf{K}]^T[\mathbf{T}]_\varepsilon^{-1},$$
$$[\eta] = [\mathbf{T}]_D[\mathbf{L}][\bar{\eta}][\mathbf{L}]^T[\mathbf{T}]_E^{-1},$$

where

$$[\mathbf{T}]_\sigma = \begin{bmatrix} \cos^2\theta & \sin^2\theta & 0 & 0 & 0 & 2\cos\theta\sin\theta \\ \sin^2\theta & \cos^2\theta & 0 & 0 & 0 & -2\cos\theta\sin\theta \\ 0 & 0 & 1 & 0 & 0 & 0 \\ 0 & 0 & 0 & \cos\theta & -\sin\theta & 0 \\ 0 & 0 & 0 & \sin\theta & \cos\theta & 0 \\ -\cos\theta\sin\theta & \cos\theta\sin\theta & 0 & 0 & 0 & \cos^2\theta-\sin^2\theta \end{bmatrix},$$

$$[\mathbf{T}]_\varepsilon = \begin{bmatrix} \cos^2\theta & \sin^2\theta & 0 & 0 & 0 & \cos\theta\sin\theta \\ \sin^2\theta & \cos^2\theta & 0 & 0 & 0 & -\cos\theta\sin\theta \\ 0 & 0 & 1 & 0 & 0 & 0 \\ 0 & 0 & 0 & \cos\theta & -\sin\theta & 0 \\ 0 & 0 & 0 & \sin\theta & \cos\theta & 0 \\ -2\cos\theta\sin\theta & 2\cos\theta\sin\theta & 0 & 0 & 0 & \cos^2\theta-\sin^2\theta \end{bmatrix},$$

$$[\boldsymbol{T}]_E = [\boldsymbol{T}]_D = \begin{bmatrix} \cos\theta & \sin\theta & 0 \\ -\sin\theta & \cos\theta & 0 \\ 0 & 0 & 1 \end{bmatrix},$$

$$[\mathbf{L}] = \begin{bmatrix} l_{11} & l_{12} & l_{13} \\ l_{21} & l_{22} & l_{23} \\ l_{31} & l_{32} & l_{33} \end{bmatrix} = \begin{bmatrix} \cos\gamma & 0 & -\sin\gamma \\ 0 & 1 & 0 \\ \sin\gamma & 0 & \cos\gamma \end{bmatrix},$$

$$[\mathbf{K}] = \begin{bmatrix} \mathbf{K}_1 & 2\mathbf{K}_2 \\ \mathbf{K}_3 & \mathbf{K}_4 \end{bmatrix},$$

$$\mathbf{K}_1 = \begin{bmatrix} l_{11}^2 & l_{12}^2 & l_{13}^2 \\ l_{21}^2 & l_{22}^2 & l_{23}^2 \\ l_{31}^2 & l_{32}^2 & l_{33}^2 \end{bmatrix}, \quad \mathbf{K}_2 = \begin{bmatrix} l_{12}l_{13} & l_{13}l_{11} & l_{11}l_{12} \\ l_{22}l_{23} & l_{23}l_{21} & l_{21}l_{22} \\ l_{32}l_{33} & l_{33}l_{31} & l_{31}l_{32} \end{bmatrix},$$

$$\mathbf{K}_3 = \begin{bmatrix} l_{21}l_{31} & l_{22}l_{32} & l_{23}l_{33} \\ l_{31}l_{11} & l_{32}l_{12} & l_{33}l_{13} \\ l_{11}l_{21} & l_{12}l_{22} & l_{13}l_{23} \end{bmatrix},$$

$$\mathbf{K}_4 = \begin{bmatrix} l_{22}l_{33}+l_{23}l_{32} & l_{23}l_{31}+l_{21}l_{33} & l_{21}l_{32}+l_{22}l_{31} \\ l_{32}l_{13}+l_{33}l_{12} & l_{33}l_{11}+l_{31}l_{13} & l_{31}l_{12}+l_{32}l_{11} \\ l_{12}l_{23}+l_{13}l_{22} & l_{13}l_{21}+l_{11}l_{23} & l_{11}l_{22}+l_{12}l_{21} \end{bmatrix}.$$

References

[1] Williams ML. Stress singularities resulting from various boundary conditions in angular corners of plates under bending. In: Proceeding of first U.S. national congress of applied mechanics; 1952. p. 325–29.

[2] Williams ML. Stress singularities resulting from various boundary conditions in angular corners of plates in extension. J Appl Mech 1952;19(4):526–8.

[3] Hartranft RJ, Sih GC. The use of eigenfunction expansions in the general solution of three-dimensional crack problems. J Math Mech 1969;19(2):123–38.

[4] Hein VL, Erdogan F. Stress singularities in a two-material wedge. Int J Fract Mech 1971;7(3):317–30.

[5] Bogy DB, Wang KC. Stress singularities at interface corners in bonded dissimilar isotropic elastic materials. Int J Solids Struct 1971;7(10):993–1005.

[6] Dempsey JP, Sinclair GB. On the stress singularities in the plate elasticity of the composite wedge. J Elasticity 1979;9(4):373–91.

[7] Dempsey JP, Sinclair GB. On the stress singular behavior at the vertex of a bi-material wedge. J Elasticity 1981;11(3):317–27.

[8] Ting TCT, Chou SC. Edge singularities in anisotropic composites. Int J Solids Struct 1981;17(11):1057–68.

[9] Ojikutu IO, Low RO, Scott RA. Stress singularities in laminated composite wedge. Int J Solids Struct 1984;20(8):777–90.

[10] Burton WS, Sinclair GB. On the singularities in Reissner's theory for the bending of elastic plates. J Appl Mech 1986;53(1):220–2.

[11] Xie M, Chaudhuri RA. Three-dimensional stress singularity at a bimaterial interface crack front. Comp Struct 1998;40(2):137–47.

[12] Huang CS. Stress singularities at angular corners in first-order shear deformation plate theory. Int J Mech Sci 2003;45(1):1–20.

[13] Huang CS, Chang MJ. Corner stress singularities in a FGM thin plate. Int J Solids Struct 2007;44(9):2802–19.

[14] Xu XL, Rajapakse RKND. On singularities in composite piezoelectric wedges and junctions. Int J Solids Struct 2000;37(23):3235–75.

[15] Hwu C, Ikeda T. Eletromechanical fracture analysis for corners and cracks in piezoelectric materials. Int J Solids Struct 2008;45(22–23):5744–64.

[16] Chue CH, Chen CD. Decoupled formulation of piezoelectric elasticity under generalized plane deformation and its application to wedge problems. Int J Solids Struct 2002;39:3131–58.

[17] Chue CH, Chen CD. Antiplane stress singularities in a bonded bimaterial piezoelectric wedge. Arch Appl Mech 2003;72(9):673–85.

[18] Chen TH, Chue CH, Lee HT. Stress singularities near the apex of a cylindrically polarized piezoelectric wedge. Arch Appl Mech 2004;74(3–4):248–61.

[19] Zak AR. Stresses in the vicinity of boundary discontinuities in bodies of revolution. ASME J Appl Mech 1964;31:150–2.

[20] Love AEH. A treatise on the mathematical theory of elasticity. 4th ed. New York: The Macmillan Co; 1927.

[21] Li YL, Hu SY, Munz D, Yang YY. Asymptotic description of the stress field around the bond edge of a cylindrical joint. Arch Appl Mech 1998;68(7):552–65.

[22] Li YL, Hu SY, Yang YY. Stresses around the bond edges of axisymmetric deformation joints. Fract Mech 2000;66(2):153–70.

[23] Timoshenko SP, Goodier JN. Axisymmetric stress and deformation in a solid of revolution. In: Theory of elasticity. Kogakusha: McGraw-Hill; 1970. p. 428–9.

[24] Ting TCT, Jin Y, Chou SC. Eigenfunctions at a singular point in transversely isotropic materials under axisymmetric deformations. ASME J Appl Mech 1985;52(3):565–9.

[25] Huang CS, Leissa AW. Three-dimensional sharp corner displacement functions for bodies of revolution. ASME J Appl Mech 2007;74(1):41–6.

[26] Huang CS, Leissa AW. Stress singularities in bimaterial bodies of revolution. Comp Struct 2008;82(4):488–98.

[27] Xu JQ, Mutoh Y. Singularity at the interface edge of bonded transversely isotropic piezoelectric dissimilar materials. JSME Int J Ser A 2001;44(4):556–66.

[28] Ding HJ, Chen B, Liang J. General solutions for coupled equations for piezoelectric media. Int J Solids Struct 1996;33(16):2283–98.

[29] Li Y, Sato Y, Watanabe K. Stress singularity analysis of axisymmetric piezoelectric bonded structure. JSME Int J Ser A 2002;45(3):363–70.

[30] Haojiang D, Weiqiu C. Three dimensional problems of piezoelasticity. New York: Nova Science Publishers Inc.; 2001.

[31] Müller DE. A method for solving algebraic equations using an automatic computer. Math Tables Aids Comput 1956;10(56):208–15.